

See discussions, stats, and author profiles for this publication at: <https://www.researchgate.net/publication/257531197>

Thermochemistry and Kinetics for 2-Butanone-1-yl Radical (CH_2 center dot $\text{C}(=\text{O})\text{CH}_2\text{CH}_3$) Reactions with O_2

ARTICLE in THE JOURNAL OF PHYSICAL CHEMISTRY A · OCTOBER 2013

Impact Factor: 2.69 · DOI: 10.1021/jp408708u · Source: PubMed

CITATIONS

7

READS

82

3 AUTHORS:



Nadia Sebbar

Karlsruhe Institute of Technology

26 PUBLICATIONS 236 CITATIONS

[SEE PROFILE](#)



Joseph W. Bozzelli

New Jersey Institute of Technology

277 PUBLICATIONS 5,264 CITATIONS

[SEE PROFILE](#)



Henning Bockhorn

Karlsruhe Institute of Technology

360 PUBLICATIONS 3,690 CITATIONS

[SEE PROFILE](#)

Thermochemistry and Kinetics for 2-Butanone-1-yl Radical ($\text{CH}_2\cdot\text{C}(=\text{O})\text{CH}_2\text{CH}_3$) Reactions with O_2

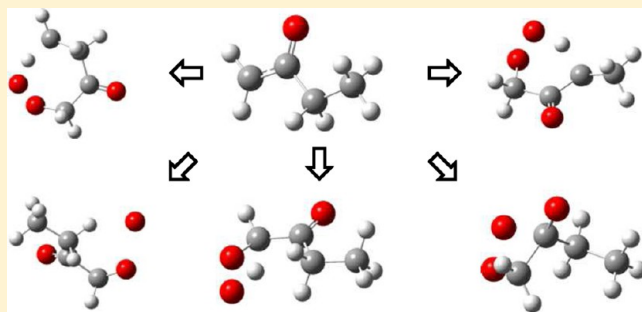
N. Sebbar,[†] J. W. Bozzelli,^{‡,*} and H. Bockhorn[†]

[†]KIT, Karlsruhe Institute of Technology, Engler-Bunte-Institut, Verbrennungstechnik Engler-Bunte Ring 1, D-76131 Karlsruhe, Germany

[‡]Department of Chemical Engineering, Chemistry and Environmental Science, New Jersey Institute of Technology, Newark, New Jersey 07102, United States

Supporting Information

ABSTRACT: Thermochemistry of reactants, intermediates, transition state structures, and products along with kinetics on the association of $\text{CH}_2\cdot\text{C}(=\text{O})\text{CH}_2\text{CH}_3$ (2-butanone-1-yl) with O_2 and dissociation of the peroxy adduct isomers are studied. Thermochemical properties are determined using ab initio (G3MP2B3 and G3) composite methods along with density functional theory (B3LYP/6-311g(d,p)). Entropy and heat capacity contributions versus temperature are determined from structures, vibration frequencies, and internal rotor potentials. The $\text{CH}_2\cdot\text{C}(=\text{O})\text{CH}_2\text{CH}_3$ radical + O_2 association results in a chemically activated peroxy radical with 27 kcal mol⁻¹ excess of energy. The chemically activated adduct can react to stabilized peroxy or hydroperoxide alkyl radical adducts, further react to lactones plus hydroxyl radical, or form olefinic ketones and a hydroperoxy radical. Kinetic parameters are determined from the G3 composite methods derived thermochemical parameters, and quantum Rice–Ramsperger–Kassel (QRRK) analysis to calculate $k(E)$ with master equation analysis to evaluate falloff in the chemically activated and dissociation reactions. One new, not previously reported, peroxy chemistry reaction is presented. It has a low barrier path and involves a concerted reaction resulting in olefin formation, H_2O elimination, and an alkoxy radical.



INTRODUCTION

Ketones are a major class of organic chemicals and are widely used as solvents. They are important in the chemistry of the atmosphere and in combustion systems from direct emissions and as intermediates. Their photodissociation in the lower atmosphere results in formation of free radicals and may influence the atmospheric oxidation capacity. Ketones are also used as fuel tracers for monitoring fuel properties, such as concentration, temperature, density, pressure, velocity, and distribution, using laser-induced fluorescence^{1,2} and as fuel additives in reducing soot emissions.^{3,4}

Carbonyls are known to be important intermediates in pyrolysis and combustion processes on saturated and unsaturated hydrocarbons. Wolfe et al.,⁵ for example, have shown in experimental studies that significant fractions of aldehydes and ketones are formed in the oxidation of isoprene. They suggest amplification of hydroxyl radical production by a possible factor of 3. Important atmospheric and combustion loss processes for ketones involve hydrogen abstractions by OH radicals, a process that is partially controlled by carbon–hydrogen bond energies, and by photolysis resulting from absorption by the carbonyl group.^{6–9} The photolysis is reported to account for significant overall global presence of OH and HO₂ radicals, particularly in the upper troposphere.^{10,11}

There are some limited studies on the chemical fate of fuel tracers, such as acetone and 3-pentanone, in hot oxidizing atmospheres.¹² Serinyel et al.¹³ for example, have published on the combustion kinetics of 3-pentanone and used thermochemistry and kinetic parameters corresponding to studies on acetone in their model development.

Several studies on the fundamental thermochemistry of the intermediate radicals on ketones or their elementary oxidation kinetics have recently appeared. Sebbar et al.¹⁴ published on the thermochemistry of 2-butanone and show that although the primary C–H bond on butanone adjacent to the carbonyl is similar to acetone, the secondary C–H bond energy is more than 5 kcal mol⁻¹ weaker. Hudzik and Bozzelli¹⁵ have also reported on thermochemical parameters of series of ketones as a function of temperature and reveal problems with matching entropy and heat capacity experimental data with vibration analysis using only frequencies from DFT and ab initio methods. They show that inclusion of internal rotor analysis and the use of the Rotator program of Lay et al.¹⁶ was required to agree with experimental entropy and heat capacity data. Sebbar et al.¹⁴ also studied the

Received: August 30, 2013

Revised: October 2, 2013

Published: October 8, 2013

Table 1. Enthalpies of Formation for Stable and Radical Species Used in Work Reactions

species	$\Delta_f H_{298}^0$ (kcal mol ⁻¹)	source	species	$\Delta_f H_{298}^0$ (kcal mol ⁻¹)	source
CH ₄	-17.89 ± 0.07	29	CH ₃ C(=O)CH ₂ CH ₃	-57.02 ± 0.20	45
CH ₃ CH ₃	-20.24 ± 0.12	29	CH ₃ CH=O	-40.80 ± 0.35	46
C ₃ H ₈	-24.82 ± 0.14	29	CH ₃ CH ₂ CH=O	-45.09 ± 0.18	46
CH ₂ =CH ₂	12.55 ± 0.1	30	CH ₃ C(=O)CH ₃	-51.9 ± 0.12	45
CH ₃ CH=CH ₂	4.879	31	HOCH ₂ CH=O	-74.54 (B3LYP)	this work
CH ₂ =C=CH ₂	116.77	GA		-73.67 (G3MP2B3)	this work
CH ₃ CH=CHCH ₃	-1.83 ± 0.30	32	CH ₃ CH ₂ C≡CH	-73.72 (G3)	this work
CH ₂ =C=CHCH ₃	38.77 ± 0.14	32	furan	39.48 ± 0.21	32
CH ₂ =C=O	-20.85	33	Y(C ₃ H ₄ O)=O	-8.29	47
CH ₂ =O	-26.24 ± 0.44	34	CH ₂ CH ₂ OCH ₃	-67.61 ± 0.2	48
CH ₂ =CHCH=O	-18.65 ± 0.95	35	CH ₂ =CHCH ₂ CH=O	-51.73 ± 0.16	49
O=CHCH=O	50.66 ± 0.19	36	H ₂ O	-20.62 ± 0.74	35
CH ₃ OH	-48.08 ± 0.05	37	HO·	-57.77	30
CH ₃ CH ₂ OH	-56.23 ± 0.12	37	CH ₃ ·	8.93 ± 0.03	50
CH ₃ CH=CHOH	-34.7	38	CH ₃ CH ₂ ·	34.821	30
CH ₃ OOH	-31.8 ± 0.94	39	CH ₃ O·	28.4 ± 0.5	51
CH ₃ CH ₂ OOH	-39.28 ± 0.01	40	CH ₂ OOH	4.1 ± 1.	51
CH ₃ CH ₂ CH ₂ OH	-61.2 ± 0.7	41	CH ₃ CH ₂ O·	15.16 ± 1.15	14
CH ₂ =Y(COCH ₃)	6.33	38	CH ₃ OO·	-2.03 ± 0.39	40
Y(CH ₂ COO)=O	-35.92 ± 0.42	42	CH ₃ CH ₂ OO·	2.15 ± 1.22	51
Y(CH ₂ CH ₂ C)=O	-14.27	GA	CH ₂ =CHCH ₂ OO·	-6.5 ± 2.36	52
CH ₂ =C(CH ₃)OH	-40.4	43	Y(C ₂ H ₄ O ₂)	20.61 ± 1.08	40
CH ₂ =C=CHCH ₃	38.77 ± 0.14	32		10.26	53
Y(C ₄ H ₈ O)	-44.03 ± 0.17	44			

oxidation kinetics of the secondary butanone radical with the O₂ reaction system and show that stabilization of the peroxy adduct and its further reactions are a major path under atmospheric conditions, and formation of olefinic ketone and HO₂ radical become important at higher temperatures.

In this study, the thermochemistry of reaction intermediates and reaction paths of the 2-butanone-1-yl radical, CH₂·C(=O)CH₂CH₃ + O₂ are determined. Structures and enthalpies of formation for important intermediate radicals, products, and transition state barriers resulting from the reaction paths of this system are reported. Standard enthalpies, $\Delta_f H_{298}^0$, are calculated using ab initio and density functional calculations and group additivity (GA).

Kinetics and important intermediates for reaction paths are determined using bimolecular chemical activation analysis as a function of temperature and pressure. High pressure limit kinetic parameters are obtained from canonical transition state theory calculations. Multifrequency quantum Rice–Ramsperger–Kassel (QRRK) analysis is used to calculate $k(E)$ data, and master equation analysis is applied to evaluate falloff in the chemically activated and dissociation reactions.

COMPUTATIONAL METHODS

Molecular properties of reactants, intermediate adducts, transition state structures and products in the CH₂·C(=O)-CH₂CH₃ + O₂ reaction system are calculated using the Gaussian 03 program suite^{17–19} with DFT at (B3LYP/6-311G(d,p)),^{20–22} G3,²³ G3MP2B3,^{24,25} and group additivity.^{26,27} A detailed description of the methods is given in our previous work.¹⁴

Contributions to entropy and heat capacity are determined from structure and vibration frequency data using the SMCPS program,²⁸ and contributions from intramolecular rotations are determined using the Rotator program.¹⁶

Standard enthalpies are determined using work reactions in which the bonding environment of both reactants and products

is similar to cancel systematic calculation errors. Enthalpies of formation of transition state structures were obtained from the computational enthalpy of activation and from the calculated enthalpies of formation of the reactants or products.

Nomenclature in this work is as follows: Y(A) indicates a cyclic structure, A· represents a radical site on the structure, TS is a transition state structure.

RESULTS AND DISCUSSION

1. Enthalpy of Formation, $\Delta_f H_{298}^0$ Calculations. Enthalpy values for standard reference species used in the work reactions are listed in Table 1, along with literature references. Standard enthalpies of formation for reactants, transition states, and products of the CH₂·C(=O)CH₂CH₃ + O₂ reaction system as well as their structures and the work reactions used are calculated and reported in Tables 2 and 3.

Comparison of the enthalpy values of the 24 radicals and stable species reported in Table 2 shows excellent agreement between G3MP2B3 and G3 using different work reactions. Differences between the two methods is less than 1 kcal mol⁻¹ for the nine stable species and for most of the radicals. There are four radicals that deviate by less than 2 kcal mol⁻¹ between the two methods. Table 2 shows a reasonable agreement between GA and B3LYP and/or G3MP2B3 and G3 calculated values. The difference between DFT and G3 and G3MP2B3 is: < 1 kcal mol⁻¹ for 7 species, < 2 kcal mol⁻¹ for 6 species and < 3 kcal mol⁻¹ for 7 species. Overall the DFT calculations show reasonable agreement with the two ab initio methods with the exception of one stable species O=CHC(OH)=CHCH₃ and the corresponding alkoxy radical CH₂(O·)C(=O)CH=CH₂ which show differences near 5 kcal mol⁻¹ from G3 and G3MP2B3. The group additivity values also show this error and surprisingly agree with the DFT data.

Estimation of the enthalpy of formation for the CH·(OOH)C(=O)CH₂CH₃ and CH·(OOH)C(OH)=CHCH₃

Table 2. Calculated $\Delta_f H_{298}^0$ for Stable Species and Radicals for the $\text{CH}_2\cdot\text{C}(=\text{O})\text{CH}_2\text{CH}_3 + \text{O}_2$ System

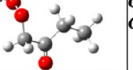
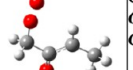
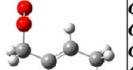
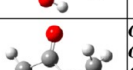
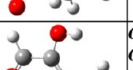
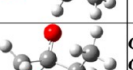
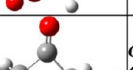
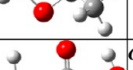
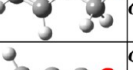
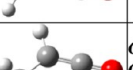
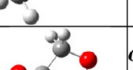
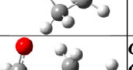
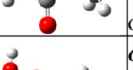
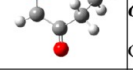
	Reactions	ΔH_{f298}^0 (kcal mol ⁻¹)			
		B3LYP/ 6-311G(d,p)	G3MP2B3	G3	GA
	$\text{CH}_2\cdot\text{C}(=\text{O})\text{CH}_2\text{CH}_3 + \text{CH}_3\text{CH}_3 \rightarrow \text{CH}_3\text{CH}_2\cdot + \text{CH}_3\text{C}(=\text{O})\text{CH}_2\text{CH}_3$ $\text{CH}_2\cdot\text{C}(=\text{O})\text{CH}_2\text{CH}_3 + \text{CH}_4 \rightarrow \text{CH}_3\text{CH}_2\cdot + \text{CH}_3\text{C}(=\text{O})\text{CH}_3$ $\text{CH}_2\cdot\text{C}(=\text{O})\text{CH}_2\text{CH}_3 + \text{H}_2 \rightarrow \text{CH}_3\text{CH}_2\cdot + \text{CH}_3\text{C}(=\text{O})\text{CH}_2\text{CH}_3$ Average	-12.73 -12.88 -15.83 -12.80 ± 2.14	-13.39 -13.76 -15.78 -13.57 ± 1.57	-13.25 -13.66 -14.86 -13.45 ± 1.02	-12.93
	$\text{CH}_2(\text{OO}\cdot)\text{C}(=\text{O})\text{CH}_2\text{CH}_3 + \text{CH}_4 \rightarrow \text{CH}_3\text{C}(=\text{O})\text{CH}_3 + \text{CH}_3\text{CH}_2\text{OO}\cdot$ $\text{CH}_2(\text{OO}\cdot)\text{C}(=\text{O})\text{CH}_2\text{CH}_3 + \text{CH}_3\text{CH}_3 \rightarrow \text{CH}_3\text{C}(=\text{O})\text{CH}_2\text{CH}_3 + \text{CH}_3\text{CH}_2\text{OO}\cdot$ $\text{CH}_2(\text{OO}\cdot)\text{C}(=\text{O})\text{CH}_2\text{CH}_3 + \text{CH}_3\text{CH}_3 \rightarrow \text{CH}_2(\text{OOH})\text{C}(=\text{O})\text{CH}_2\text{CH}_3 + \text{CH}_3\text{CH}_2\cdot$ Average	-39.77 -41.84 -42.66 -41.42 ± 1.49	-39.71 -40.79 -40.05 -40.18 ± 0.55	-39.91 -40.88 -40.78 -40.52 ± 0.53	-37.97
	$\text{CH}_2(\text{OOH})\text{C}(=\text{O})\text{CH}_2\text{CH}_3 + \text{CH}_4 \rightarrow \text{CH}_3\text{CH}_2\text{C}(=\text{O})\text{CH}_3 + \text{CH}_3\text{OOH}$ $\text{CH}_2(\text{OOH})\text{C}(=\text{O})\text{CH}_2\text{CH}_3 + \text{CH}_3\text{CH}_3 \rightarrow \text{CH}_3\text{C}(=\text{O})\text{CH}_2\text{CH}_3 + \text{CH}_3\text{CH}_2\text{OOH}$ Average	-75.14 -76.76 -75.95 ± 1.15	-74.77 -75.58 -75.18 ± 0.57	-75.07 -75.59 -75.33 ± 0.37	-73.57
	$\text{CH}_2(\text{OOH})\text{C}(=\text{O})\text{CH}\cdot\text{CH}_3 + \text{H}_2 \rightarrow \text{CH}_3\text{CH}_2\cdot + \text{CH}_3\text{C}(=\text{O})\text{CH}_3 + \text{CH}_3\text{OOH}$ $\text{CH}_2(\text{OOH})\text{C}(=\text{O})\text{CH}\cdot\text{CH}_3 + \text{H}_2 + \text{CH}_3\text{CH}_3 \rightarrow \text{CH}_3\text{CH}_2\cdot + \text{CH}_3\text{C}(=\text{O})\text{O} + \text{CH}_3\text{OOH}$ $\text{CH}_2(\text{OOH})\text{C}(=\text{O})\text{CH}\cdot\text{CH}_3 + \text{CH}_3\text{CH}_3 \rightarrow \text{CH}_2(\text{OOH})\text{C}(=\text{O})\text{CH}_2\text{CH}_3 + \text{CH}_3\text{CH}_2\cdot$ Average	-39.34 -41.12 -38.57 -39.68 ± 1.31	-37.87 -38.60 -36.63 -37.70 ± 1.0	-37.06 -38.04 -36.84 -37.31 ± 0.64	-37.67
	$\text{CH}_2(\text{OOH})\text{C}(=\text{O})\text{CH}_2\text{CH}_2\cdot + \text{C}_3\text{H}_8 + \text{H}_2 \rightarrow \text{CH}_3\text{CH}_2\cdot + \text{CH}_3\text{CH}_2\text{C}(=\text{O})\text{CH}_3 + \text{CH}_3\text{OOH}$ $\text{CH}_2(\text{OOH})\text{C}(=\text{O})\text{CH}_2\text{CH}_2\cdot + \text{H}_2 + \text{CH}_3\text{CH}_3 \rightarrow \text{CH}_3\text{CH}_2\cdot + \text{CH}_3\text{C}(=\text{O})\text{CH}_3 + \text{CH}_3\text{OOH}$ $\text{CH}_2(\text{OOH})\text{C}(=\text{O})\text{CH}_2\text{CH}_2\cdot + \text{CH}_3\text{CH}_3 \rightarrow \text{CH}_2(\text{OOH})\text{C}(=\text{O})\text{CH}_2\text{CH}_3 + \text{CH}_3\text{CH}_2\cdot$ Average	-28.04 -27.98 -27.22 -27.75 ± 0.46	-27.86 -27.75 -26.51 -27.37 ± 0.75	-27.08 -27.02 -26.79 -26.96 ± 0.15	-24.67
	$\text{CH}_2(\text{OO}\cdot)\text{C(OH)}=\text{CHCH}_3 + \text{C}_3\text{H}_8 + \text{H}_2 \rightarrow \text{CH}_3\text{CH}_2\text{OH} + \text{CH}_3\text{CH}=\text{CHCH}_3 + \text{CH}_3\text{OO}\cdot$ $\text{CH}_2(\text{OO}\cdot)\text{C(OH)}=\text{CHCH}_3 + \text{CH}_4 \rightarrow \text{CH}_3\text{CH}=\text{CHOH} + \text{CH}_3\text{CH}_2\text{OO}\cdot$ $\text{CH}_2(\text{OO}\cdot)\text{C(OH)}=\text{CHCH}_3 + \text{H}_2 \rightarrow \text{CH}_2=\text{CHOH} + \text{CH}_3\text{CH}_2\text{OO}\cdot$ $\text{CH}_2(\text{OO}\cdot)\text{C(OH)}=\text{CHCH}_3 + \text{CH}_4 \rightarrow \text{CH}_2=\text{CHCH}_2\text{OO}\cdot + \text{CH}_3\text{CH}_2\text{OH}$ Average	-31.43 -28.18 -32.23 -30.80 -30.61 ± 1.75	-29.47 -27.82 -30.97 -27.18 -29.42 ± 1.82	-28.99 -28.15 -30.27 -28.91 -29.14 ± 0.88	-28.63
	$\text{O}=\text{CHC}(=\text{O})\text{CH}_2\text{CH}_3 + \text{H}_2 \rightarrow \text{CH}_3\text{CH}_3 + \text{O}=\text{CHCH}=\text{O}$ $\text{O}=\text{CHC}(=\text{O})\text{CH}_2\text{CH}_3 + \text{CH}_3\text{CH}_3 \rightarrow \text{CH}_3\text{CH}_2\text{CH}=\text{O} + \text{CH}_3\text{C}(=\text{O})\text{CH}_3$ $\text{O}=\text{CHC}(=\text{O})\text{CH}_2\text{CH}_3 + \text{H}_2 \rightarrow \text{CH}_3\text{CH}_3 + \text{O}=\text{CHCH}=\text{O}$ Average	-72.46 -72.09 -72.46 -72.34 ± 0.21	-71.15 -72.08 -71.15 -71.46 ± 0.54	-70.42 -72.08 -70.42 -70.97 ± 0.96	-69.8
	$\text{O}=\text{CHC(OH)}=\text{CHCH}_3 + \text{C}_3\text{H}_8 + \text{H}_2 \rightarrow \text{CH}_3\text{CH}_2\text{OH} + \text{CH}_3\text{CH}=\text{O} + \text{CH}_2=\text{CHCH}_3$ $\text{O}=\text{CHC(OH)}=\text{CHCH}_3 + \text{CH}_4 \rightarrow \text{CH}_2=\text{CHCH}_2\text{CH}=\text{O} + \text{CH}_3\text{OH}$ $\text{O}=\text{CHC(OH)}=\text{CHCH}_3 + \text{CH}_3\text{CH}_3 \rightarrow \text{CH}_2=\text{CHCH}=\text{O} + \text{CH}_3\text{CH}_2\text{CH}_2\text{OH}$ Average	-71.42 -70.96 -69.17 -70.52 ± 1.19	-66.45 -64.95 -65.99 -65.80 ± 0.77	-66.13 -67.29 -65.68 -66.36 ± 0.83	-72.01
	$\text{CH}_3\text{CH}_2\text{Y}(\text{C}(\text{O}\cdot)\text{CH}_2\text{OO}) + \text{H}_2 + \text{CH}_3\text{CH}_3 \rightarrow \text{Y}(\text{CH}_2\text{CH}_2\text{OO}) + \text{CH}_3\text{O}\cdot + \text{CH}_2=\text{CHCH}=\text{O}$ $\text{CH}_3\text{CH}_2\text{Y}(\text{C}(\text{O}\cdot)\text{CH}_2\text{OO}) \rightarrow \text{CH}_3\text{CH}_2\cdot + \text{Y}(\text{CH}_2\text{OOC}=\text{O})$ Average	-7.00 - -7.00	-8.43 -6.86 -7.64 ± 1.11	-7.11 -6.60 -6.85 ± 0.36	-6.95
	$\text{CH}_3\text{Y}(\text{CHOCH}_2\text{C}(=\text{O})) + \text{CH}_4 \rightarrow \text{Y}(\text{CH}_2\text{CH}_2\text{OC}(=\text{O})) + \text{CH}_3\text{CH}_3$ $\text{CH}_3\text{Y}(\text{CHOCH}_2\text{C}(=\text{O})) + \text{H}_2 + \text{CH}_3\text{CH}_3 \rightarrow \text{CH}_3\text{CH}_2\text{OCH}_3 + \text{CH}_3\text{C}(=\text{O})\text{CH}_3$ Average	-50.60 -60.54 -55.57 ± 7.03	-51.88 -54.86 -53.37 ± 2.11	-53.79 -54.00 -53.89 ± 0.15	-50.68
	$\text{CH}_2=\text{CHC}(=\text{O})\text{CH}_2\text{OH} + \text{CH}_3\text{CH}_3 + \text{H}_2 \rightarrow \text{CH}_3\text{OH} + \text{CH}_3\text{C}(=\text{O})\text{CH}_3 + \text{CH}_2=\text{CH}_2$ $\text{CH}_2=\text{CHC}(=\text{O})\text{CH}_2\text{OH} + \text{H}_2 \rightarrow \text{CH}_2=\text{CHCH}=\text{O} + \text{CH}_3\text{OH}$ $\text{CH}_2=\text{CHC}(=\text{O})\text{CH}_2\text{OH} + \text{H}_2 \rightarrow \text{OHCH}_2\text{CH}=\text{O} + \text{CH}_2=\text{CH}_2$ Average	-67.27 -68.21 -68.08 -67.85 ± 0.51	-64.67 -65.56 -65.61 -65.28 ± 0.53	-64.08 -65.45 -65.30 -64.94 ± 0.75	-63.19
	$\text{CH}_2=\text{C}=\text{O} + \text{CH}_4 \rightarrow \text{CH}_2=\text{CH}_2 + \text{CH}_2=\text{C}=\text{O}$ $\text{CH}_2=\text{C}=\text{O} + \text{CH}_2=\text{CH}_2 \rightarrow \text{CH}_2=\text{C}=\text{CH}_2 + \text{CH}_2=\text{C}=\text{O}$ Average	18.24 13.07 15.66 ± 3.66	22.19 15.16 18.68 ± 4.97	-	-
	$\text{CH}_3\text{CH}=\text{C}=\text{O} + \text{CH}_2=\text{CH}_2 \rightarrow \text{CH}_3\text{CH}=\text{CH}_2 + \text{CH}_2=\text{C}=\text{O}$ $\text{CH}_3\text{CH}=\text{C}=\text{O} + \text{CH}_4 \rightarrow \text{CH}_3\text{CH}_3 + \text{CH}_2=\text{C}=\text{O}$ Average	-24.75 -24.41 -24.58 ± 0.24	-24.37 -24.34 -24.35 ± 0.02	-24.47 -24.52 -24.50 ± 0.04	-22.46
	$\text{O}=\text{Y}(\text{CCH}_2\text{CH}_2\text{OCH}_2) + \text{CH}_3\text{CH}_3 + \text{H}_2 \rightarrow \text{CH}_3\text{C}(=\text{O})\text{CH}_3 + \text{CH}_3\text{CH}_2\text{OCH}_3$ $\text{O}=\text{Y}(\text{CCH}_2\text{CH}_2\text{OCH}_2) + \text{CH}_3\text{CH}_2\text{CH}_3 \rightarrow \text{Y}(\text{C}_4\text{H}_8\text{O}) + \text{CH}_3\text{C}(=\text{O})\text{CH}_3$ Average	-72.74 -70.04 -71.37 ± 1.91	-69.39 -69.67 -69.53 ± 0.20	-68.55 -69.71 -69.13 ± 0.82	-67.81
	$\text{CH}_2(\text{O}\cdot)\text{C}(=\text{O})\text{CH}_2\text{CH}_3 + \text{CH}_4 \rightarrow \text{CH}_3\text{C}(=\text{O})\text{CH}_3 + \text{CH}_3\text{CH}_2\text{O}\cdot$ $\text{CH}_2(\text{O}\cdot)\text{C}(=\text{O})\text{CH}_2\text{CH}_3 + \text{CH}_3\text{CH}_3 \rightarrow \text{CH}_3\text{C}(=\text{O})\text{CH}_2\text{CH}_3 + \text{CH}_3\text{CH}_2\text{O}\cdot$ Average GA from RMG [Error! Bookmark not defined.] = -38.02 kcal mol ⁻¹	-41.12 -43.19 -42.16 ± 1.46	-37.73 -41.70 -39.71 ± 2.81	-39.01 -42.88 -40.94 ± 2.74	-37.71
	$\text{CH}\cdot(\text{OOH})\text{C}(=\text{O})\text{CH}_2\text{CH}_3 + \text{H}_2 \rightarrow \text{CH}_3\text{CH}_2\text{CH}=\text{O} + \text{CH}_2\cdot\text{OOH}$ $\text{CH}\cdot(\text{OOH})\text{C}(=\text{O})\text{CH}_2\text{CH}_3 + \text{CH}_3\text{CH}_3 \rightarrow \text{CH}_3\text{CH}_2\cdot + \text{CH}_2(\text{OOH})\text{C}(=\text{O})\text{CH}_2\text{CH}_3$ $\text{CH}\cdot(\text{OOH})\text{C}(=\text{O})\text{CH}_2\text{CH}_3 + \text{CH}_4 \rightarrow \text{CH}_3\text{CH}_2\text{C}(=\text{O})\text{CH}_3 + \text{CH}_2\cdot\text{OOH}$ Average GA from RMG [Error! Bookmark not defined.] = -28.69 kcal mol ⁻¹	unstable, decomposes to: -39.20 -39.09 -39.10 -39.13 ± 0.06			-32.07
	$\text{CH}\cdot(\text{OOH})\text{C}(\text{O}\cdot)=\text{CHCH}_3 + \text{H}_2 \rightarrow \text{CH}_3\text{CH}_2\text{CH}=\text{O} + \text{CH}_2\cdot\text{OOH}$ $\text{CH}\cdot(\text{OOH})\text{C}(\text{O}\cdot)=\text{CHCH}_3 + \text{CH}_3\text{CH}_3 \rightarrow \text{CH}_3\text{CH}_2\cdot + \text{CH}_2(\text{OOH})\text{C}(=\text{O})\text{CH}_2\text{CH}_3$ $\text{CH}\cdot(\text{OOH})\text{C}(\text{O}\cdot)=\text{CHCH}_3 + \text{CH}_4 \rightarrow \text{CH}_3\text{CH}_2\text{C}(=\text{O})\text{CH}_3 + \text{CH}_2\cdot\text{OOH}$ Average GA from RMG [Error! Bookmark not defined.] = -28.96	unstable, decomposes to: -27.80 -28.33 -28.91 -28.35 ± 0.56			-22.73
	$\text{CH}_2(\text{OOH})\text{C}(\text{O}\cdot)\text{CH}=\text{CH}_2 + 3\text{H}_2 + \text{CH}_4 \rightarrow \text{CH}_2\text{CH}_2 + \text{CH}_3\text{OOH} + \text{CH}_3\text{CH}\cdot\text{OH}$ $\text{CH}_2(\text{OOH})\text{C}(\text{O}\cdot)\text{CH}=\text{CH}_2 + 2\text{C}_2\text{H}_6 \rightarrow \text{CH}_3\text{CH}_2\text{CH}=\text{CH}_2 + \text{CH}_3\text{CH}_2\text{OOH} + \text{CH}_3\text{CH}\cdot\text{OH}$ Average GA from RMG [Error! Bookmark not defined.] = -28.84	-34.17 -30.93 -32.55 ± 2.29	-30.34 -30.01 -30.18 ± 0.23	-31.21 -31.74 -31.47 ± 0.37	-27.65

Table 2. continued

	Reactions	$\Delta H_{f,298}^0$ (kcal mol ⁻¹)			
		B3LYP/ 6-311G(d,p)	G3MP2B3	G3	GA
	$CH_2\bullet C(OH)=CHCH_3 + CH_4 \rightarrow CH_3CH_2OH + CH_2\bullet CH=CH_2$ $CH_2\bullet C(OH)=CHCH_3 + CH_3CH_3 \rightarrow CH_2\bullet CH_2OH + CH_3CH=CHCH_3$ $CH_2\bullet C(OH)=CHCH_3 + CH_4 \rightarrow CH_3CH=CHOH + CH_3CH_2\bullet$	-11.51 -10.09 -9.49	-8.94 -7.42 -8.41	-8.68 -8.31 -9.05	
	Average	-10.36 ± 1.04	-8.26 ± 0.77	-8.68 ± 0.37	-9.77
	$CH_2(OOH)C(OH)=CHCH_3\bullet + H_2 + CH_3 \rightarrow CH_2=CH_2 + CH_3OOH + CH_3CH\bullet(OH)$ $CH_2(OOH)C(OH)=CHCH_3\bullet + 2C_2H_6 \rightarrow CH_2=CHCH_2CH_3 + C_2H_5OOH + CH_3CH\bullet(OH)$	-34.17 -30.93	-30.34 -30.01	-31.21 -31.74	
	Average	-32.55 ± 2.29	-30.18 ± 0.23	-31.47 ± 0.37	
	$CH_2(OOH)C(=O)CH=CH_2 + CH_4 \rightarrow CH_3C(=O)CH=CH_2 + CH_3OOH$ $CH_2(OOH)C(=O)CH=CH_2 + CH_3CH_3 \rightarrow CH_3C(=O)CH=CH_2 + CH_3CH_2OOH$ $CH_2(OOH)C(=O)CH=CH_2 + H_2 + C_3H_8 \rightarrow CH_3C(=O)CH_3 + CH_3OOH + CH_3CH=CH_2$ $CH_2(OOH)C(=O)CH=CH_2 + CH_3CH_3 \rightarrow CH_3C(=O)CH_2CH_3 + CH_2\bullet CHOOH$	-46.55 -45.95 -46.89 -45.17	-44.70 -44.06 -45.03 -45.03	-45.35 -44.50 -44.43 -45.21	
	Average	-46.14 ± 0.75	-44.70 ± 0.46	-44.87 ± 0.47	-47.09
	$CH_2(OOH)C(OH)CH=CH_2 + 2C_2H_6 \rightarrow C_2H_5OOH + CH_2=CHCH_2CH_3 + CH_3CH\bullet OH$ $CH_2(OOH)C(OH)CH=CH_2 \rightarrow CH_2(OO\bullet)C(=O)CH_2CH_3$	-30.93 -28.23	-30.01 -30.12	-31.74 -30.42	
	Average	-29.58 ± 1.91	-30.07 ± 0.08	-31.08 ± 0.93	-27.65
	$CH_2(O\bullet)C(=O)CH=CH_2 + CH_4 \rightarrow CH_2=CHCH=O + CH_3CH_2O\bullet$ $CH_2(O\bullet)C(=O)CH=CH_2 + CH_4 + CH_3CH_3 \rightarrow CH_3C(=O)CH_3 + CH_2=CH_2 + CH_3CH_2O\bullet$	-12.13 -10.69	-6.12 -5.65	-	
	Average	-11.41 ± 1.02	-5.89 ± 0.11	-	-11.23
GA from RMG [Error! Bookmark not defined.] = -11.54					
	$CH\bullet=C(OH)CH_2CH_3 + H_2 \rightarrow CH_3CH_2OH + CH_2\bullet CH\bullet$ $CH\bullet=C(OH)CH_2CH_3 + CH_4 \rightarrow CH_2=C(CH_3)OH + CH_3CH_2\bullet$	17.12 18.99	18.94 19.54	19.70 -	
	Average	18.06 ± 1.32	19.24 ± 0.42	19.70	16.34

radicals is difficult because of the radical instability. Many higher-level calculation methods do not calculate a stable minimum, but show that the radicals dissociate (beta scission) to OH + a carbonyl, O=CHC(=O)CH₂CH₃ and OH plus O=CHC(OH)=CHCH₃, respectively (see illustration in Table 2). A typical RO-OH bond is ~45 kcal mol⁻¹, and the π bond formed in the new carbonyl group is ~80 kcal mol⁻¹, which would make this beta scission reaction 35 kcal mol⁻¹ exothermic. A number of calculation methods converge only to the stable carbonyl and OH products, not to a stable minimum. In this study, only G3 calculations with MP2 optimizations calculate a stable minimum that allows estimation of an enthalpy for these hydroperoxide carbon radicals. Estimation of the RC-O-OH bond energy should be considered with caution; the results show 23.5 kcal mol⁻¹ for CH \cdot (OOH)C(=O)CH₂CH₃ and 28.5 kcal mol⁻¹ for CH \cdot (OOH)C(OH)=CHCH₃. The standard enthalpy of CH \cdot (OOH)C(=O)CH₂CH₃ is estimated at -39.1 kcal mol⁻¹ (with G3), which when compared to a group additivity estimate (which does not consider an HO₂ group on the adjacent carbon) is off by 7 kcal mol⁻¹ and by 10 kcal mol⁻¹ when compared to an RMG value.³⁸

Table 3 lists the enthalpies ($\Delta_f H_{TS(298)}^0$) of 28 transition state structures; it also illustrates the structures to help in describing the reaction paths. The $\Delta_f H_{TS(298)}^0$ enthalpy values are calculated from both the reactant and the product. The calculation of $\Delta_f H_{TS(298)}^0$ from this difference reaction is similar to an isodesmic reaction and includes cancellation of errors for similar bonds in the reactant and TS structure. Comparison of G3 with G3MP2B3 results shows good agreement; the difference between the two ab initio methods is <1 kcal mol⁻¹ for 8 species and ≤ 2 kcal mol⁻¹ for 9 species. There are larger differences at 3.7 kcal mol⁻¹ for TS1-9, 3.9 kcal mol⁻¹ for TS5 and 5.5 kcal mol⁻¹ for TS1-4. G3MP2B3 values are recommended and marked in bold in Table 3 as the frequencies and structure are from the same method.

The reason is that we consider some B3LYP structures, used in G3MP2B3, to be likely more accurate than HF/6-31G(d) used in G3. There are significant deviations between the enthalpies for TS04 and TS1-2. Additional calculations at the G3MP2 and

CBS-APNO levels, which use MP2 and QCISD (as opposed to B3LYP) for optimized TS structures were run. For these transition state barriers, we recommend the average of G3, G3MP2, and CBS-APNO, with -4.9 kcal mol⁻¹ for TS1-2 and 22.5 kcal mol⁻¹ for TS04. The data in Table 3 show that the DFT calculation results can have lower accuracy for TS structures than for stable and radical species, where deviations from the ab initio data range from 2 to 7 kcal mol⁻¹, with larger differences of 9–12.7 kcal mol⁻¹ shown for DFT and G3MP2B3 for TS1-3, TS1-3B, TS1-5 and TS2-1.

2. Entropy $S^0(298)$ and Heat Capacities, $C_p(T)$ (300 ≤ $T/K \leq 1500$) Calculations. The entropy $S_{f,298}^0$ and heat capacity $C_{p,298}(T)$ for intermediates, transition state structures, and final products are calculated using the rigid-rotor-harmonic-oscillator approximation^{16,53} and based on the calculated parameters: frequencies, moments of inertia, symmetry, spin degeneracy, and optical isomers. These entropies and heat capacities are listed in the Supporting Information. Vibration frequencies and moments of inertia from the optimized B3LYP/6-311G(d,p) structures were used to calculate the contributions to entropy and heat capacity from vibration, translation, and external rotation (TVR) on the basis of formulas from statistical mechanics and by use of the SMCP²⁸ program. The DFT data are chosen for the stable species and the radicals because it is the same method but a larger basis set, 6-311G(d,p), than the B3LYP/6-31G(d) used in G3MP2B3 and is considered better than the HF/6-31G(d) used in G3. For the transition state structures, the G3MP2B3 data are selected. The contributions to $S_{f,298}^0$ and $C_{p,298}(T)$ from low barrier (below 6.5 kcal mol⁻¹) torsion frequencies were removed from the calculations, and contributions from internal rotations were substituted. This 6.5 kcal mol⁻¹ parameter results from our study comparing calculated entropy and heat capacity with experimental data, which will be reported in a separate publication. The torsion frequencies are identified by viewing bond motions using the GaussView program.

3. Unimolecular Reactions of the 2-Butanone-1-yl Radical $CH_2\bullet C(=O)CH_2CH_3$. Unimolecular reactions of the 2-butanone-1-yl radical are illustrated in Figure 1. The lowest reaction barrier (TS04) at 31.5 kcal mol⁻¹ is beta scission to

Table 3. Calculated $\Delta_f H_{298}^0$ of Transition State Structures

	Reactions	$\Delta_f H_{TS(298)}^0$ (kcal mol ⁻¹)		
Transition state Structure	Radical → TS → Products	B3LYP /6-311G(d,p)	G3MP2B3	G3
	$\text{CH}_2\bullet\text{C}(=\text{O})\text{CH}_2\text{CH}_3 \rightarrow \text{TS0}$ $\text{TS0} \rightarrow \text{CH}_2\bullet\text{C(OH)=CHCH}_3$	32.97 31.13 Average	36.14 37.72 36.93 ± 1.12	36.90 38.08 37.49 ± 0.83
	$\text{CH}_2\bullet\text{C(OH)=CHCH}_3 \rightarrow \text{TS01}$ $\text{TS01} \rightarrow \text{CH}_2=\text{C=CHCH}_3 + \text{OH}$	39.33 43.87 Average	44.39 45.15 44.77 ± 0.54	45.12 44.98 45.05 ± 0.1
	$\text{CH}_2\bullet\text{C}(=\text{O})\text{CH}_2\text{CH}_3 \rightarrow \text{TS02a}$ $\text{TS02a} \rightarrow \text{CH}_3\text{CH}_2\text{C(OH)=CH}\bullet$	45.07 38.98 Average	48.65 47.98 48.32 ± 0.47	47.87 - 47.87
	$\text{CH}_3\text{CH}_2\text{C(OH)=CH}\bullet \rightarrow \text{TS02}$ $\text{TS02} \rightarrow \text{CH}_3\text{CH}_2\text{C}\equiv\text{CH} + \text{OH}$	40.24 46.38 Average	46.09 48.27 47.18 ± 1.54	- 47.41 47.41 ± 0.
	$\text{CH}_2\bullet\text{C}(=\text{O})\text{CH}_2\text{CH}_3 \rightarrow \text{TS03}$ $\text{TS03} \rightarrow \text{CH}_2=\text{Y}(\text{CCH}_2\text{O}) + \text{CH}_3$	68.43 64.85 Average	72.64 65.60 69.12 ± 4.98	- -
	$\text{CH}_2\bullet\text{C}(=\text{O})\text{CH}_2\text{CH}_3 \rightarrow \text{TS04}$ $\text{TS04} \rightarrow \text{CH}_2=\text{C=O} + \text{CH}_3\text{CH}_2\bullet$	17.47 18.26 Average	22.93 - 17.87 ± 0.56	22.36 - -
G3MP2 = 21.87, CBS-APNO = 23.22				
Recommended value 22.5 (see text)				
	$\text{CH}_2(\text{OO}\bullet)\text{C}(=\text{O})\text{CH}_2\text{CH}_3 \rightarrow \text{TS1}$ $\text{TS1} \rightarrow \text{CH}_2(\text{OOH})\text{C}(=\text{O})\text{CH}\bullet\text{CH}_3$	-22.83 -25.75 Average	-17.00 -18.29 -17.65 ± 0.91	-16.52 -17.66 -17.09 ± 0.81
	$\text{CH}_2(\text{OOH})\text{C}(=\text{O})\text{CH}\bullet\text{CH}_3 \rightarrow \text{TS1-1}$ $\text{TS1-1} \rightarrow \text{CH}_3\text{Y}(\text{CHC}(=\text{O})\text{CH}_2\text{O}) + \text{OH}$	-14.37 -12.58 Average	-9.22 -4.32 -6.77 ± 3.46	- -
	$\text{CH}_3\text{Y}(\text{CHC}(=\text{O})\text{CH}_2\text{O}) \rightarrow \text{TS1-2}$ $\text{TS1-2} \rightarrow \text{CH}_2=\text{O} + \text{CH}_3\text{CH=C=O}$	CBS-APNO -4.38 -5.46 G2MP2 value = -5.32 -4.92 ± 0.7	G3MP2 -4.88	-5.00
Recommended value -4.9 (see text)				
	$\text{CH}_2(\text{OOH})\text{C}(=\text{O})\text{CH}\bullet\text{CH}_3 \rightarrow \text{TS1-3}$ $\text{TS1-3} \rightarrow \text{CH}_2=\text{CHC}(=\text{O})\text{CH}_2\text{OH} + \text{OH}$	-2.09 -2.76 Average	13.71 16.68 15.19 ± 2.10	12.89 15.02 13.95 ± 1.51
	$\text{CH}_2(\text{OOH})\text{C}(=\text{O})\text{CH}\bullet\text{CH}_3 \rightarrow \text{TS1-3B}$ $\text{TS1-3B} \rightarrow \text{CH}_2=\text{CHC}(=\text{O})\text{CH}_2\text{O}\bullet + \text{H}_2\text{O}$	-24.36 -22.02 Average	-12.82 -13.40 -13.11 ± 0.41	-
	$\text{CH}_2(\text{OOH})\text{C}(=\text{O})\text{CH}\bullet\text{CH}_3 \rightarrow \text{TS1-4}$ $\text{TS1-4} \rightarrow \text{CH}_2=\text{O} + \text{CH}_3\text{CH=C=O} + \text{OH}$	-8.85 -3.53 Average	-11.85 -5.87 -8.86 ± 4.23	-0.65 -6.16 -3.40 ± 3.90
	$\text{CH}_2(\text{OOH})\text{C}(=\text{O})\text{CH}\bullet\text{CH}_3 \rightarrow \text{TS1-5}$ $\text{TS1-5} \rightarrow \text{CH}_2(\text{OO}\bullet)\text{C(OH)=CHCH}_3$	-24.19 -25.86 Average	-13.37 -12.89 -13.13 ± 0.34	- -
	$\text{CH}_2(\text{OO}\bullet)\text{C(OH)=CHCH}_3 \rightarrow \text{TS1-6}$ $\text{TS1-6} \rightarrow \text{O=CHC(OH)=CHCH}_3 + \text{OH}$ $\text{TS1-6} \rightarrow \text{CH}\bullet(\text{OOH})\text{C(OH)=CHCH}_3$	3.00 5.72 - Average	10.17 12.37 - 11.27 ± 1.56	10.27 9.88 10.49 10.21 ± 0.31
	$\text{CH}\bullet(\text{OOH})\text{C(OH)=CHCH}_3 \rightarrow \text{TS1-7}$ $\text{TS1-7} \rightarrow \text{O=CHC(OH)=CHCH}_3 + \text{OH}$	- - - Average	- - - -28.34 ± 0.43	-28.04 -28.65

Table 3. continued

	Reactions	$\Delta_f H_{TS(298)}^0$ (kcal mol ⁻¹)		
Transition state Structure	Radical → TS → Products	B3LYP /6-311G(d,p)	G3MP2B3	G3
	$\text{CH}_2(\text{OO}\bullet) \text{CH}(\text{OH})=\text{CHCH}_3 \rightarrow \text{TS1-8}$ $\text{TS1-8} \rightarrow \text{CH}_2(\text{OOH})\text{C}(\text{OH})=\text{CHCH}_2\bullet$ Average	-14.43 -14.11 -14.27 ± 0.23	-6.97 -7.39 -7.18 ± 0.30	-4.84 -6.14 -5.49 ± 0.92
	$\text{CH}_2(\text{OOH})\text{C}\bullet(\text{OH})\text{CH}=\text{CH}_2 \rightarrow \text{TS1-9}$ $\text{TS1-9} \rightarrow \text{CH}_2=\text{C}(\text{OH})\text{CH}=\text{CH}_2 + \text{OOH}$ Average	- -8.33 -8.33	-5.66 -4.57 -5.11 ± 0.77	-8.55 -9.05 -8.80 ± 0.35
	$\text{CH}_2(\text{OOH})\text{C}\bullet(\text{OH})\text{CH}=\text{CH}_2 \rightarrow \text{TS1-10}$ $\text{TS1-10} \rightarrow \text{CH}_2(\text{OOH})\text{C}(=\text{O})\text{CH}=\text{CH}_2 + \text{H}$ Average	7.00 9.43 8.21 ± 1.12	12.85 12.62 12.73 ± 0.16	12.13 11.71 11.92 ± 0.30
	$\text{CH}_2(\text{OO}\bullet)\text{C}(=\text{O})\text{CH}_2\text{CH}_3 \rightarrow \text{TS2}$ $\text{TS2} \rightarrow \text{CH}_2(\text{OOH})\text{C}(=\text{O})\text{CH}_2\text{CH}_2\bullet$ Average	-15.61 -17.60 -16.60 ± 1.41	-10.31 -11.18 -10.74 ± 0.62	-8.60 -9.26 -8.93 ± 0.47
	$\text{CH}_2(\text{OOH})\text{C}(=\text{O})\text{CH}_2\text{CH}_2\bullet \rightarrow \text{TS2-1}$ $\text{TS2-1} \rightarrow \text{O=Y(CCH}_2\text{OCH}_2\text{CH}_2) + \text{OH}$ Average	-17.60 -19.81 -18.71 ± 1.56	-11.18 -8.12 -9.65 ± 2.13	-9.26 -6.36 -7.81 ± 2.05
	$\text{CH}_2(\text{OOH})\text{C}(=\text{O})\text{CH}_2\text{CH}_2\bullet \rightarrow \text{TS2-2}$ $\text{TS2-2} \rightarrow \text{HOOCH}_2\text{C}\bullet=\text{O} + \text{CH}_2=\text{CH}_2$ Average	-7.60 0.13 -3.73 ± 5.47	-2.71 0.04 -1.33 ± 1.94	-3.86 -1.43 -2.65 ± 1.72
	$\text{HOOCH}_2\text{C}\bullet=\text{O} \rightarrow \text{TS2-3}$ $\text{TS2-3} \rightarrow + \text{CH}_2=\text{O} + \text{OH} + \text{CO}$ Average	-11.92 -6.28 -9.10 ± 3.99	-8.53 -5.03 -6.78 ± 2.47	- - -
	$\text{CH}_2(\text{OO}\bullet)\text{C}(=\text{O})\text{CH}_2\text{CH}_3 \rightarrow \text{TS3}$ $\text{TS3} \rightarrow \text{CH}_3\text{CH}_2\text{C}(=\text{O})\text{CH}=\text{O} + \text{OH}$ $\text{TS3} \rightarrow (\text{OOH})\text{CH}\bullet\text{C}(=\text{O})\text{CH}_2\text{CH}_2$ Average	-4.73 -2.61 -3.67 ± 1.5	0.37 3.00 1.69 ± 1.86	-0.10 - -0.62 -0.36 ± 0.37
	$(\text{OOH})\text{CH}\bullet\text{C}(=\text{O})\text{CH}_2\text{CH}_2 \rightarrow \text{TS3-1}$ $\text{TS3-1} \rightarrow \text{CH}_3\text{CH}_2\text{C}(=\text{O})\text{CH}=\text{O} + \text{OH}$ Average	unstable	unstable	-37.60 -34.68 -36.14 ± 2.06
	$\text{CH}_2(\text{OO}\bullet)\text{C}(=\text{O})\text{CH}_2\text{CH}_3 \rightarrow \text{TS4}$	5.21		-
	$\text{CH}_2(\text{OO}\bullet)\text{C}(\text{OH})=\text{CHCH}_3 \rightarrow \text{TS4-1}$ $\text{TS4-1} \rightarrow \text{CH}_3\text{CH}_2\text{C}\bullet=\text{O} + \text{CH}_2=\text{O}$ Average	-38.56 -32.22 -35.39 ± 4.48	-36.89 -33.10 -35.00 ± 2.68	-37.66 -33.55 -35.61 ± 2.91
	$\text{CH}_3\text{C}(=\text{O})\text{CH}(\text{OO}\bullet)\text{CH}_3 \rightarrow \text{TS5}$ $\text{TS5} \rightarrow \text{CH}_3\text{CH}_2\text{C}(=\text{O})\text{O}\bullet + \text{CH}_2=\text{O}$ Average	-10.90 -7.85 -9.37 ± 2.16	-9.00 -7.41 -8.20 ± 1.12	-2.15 -6.29 -4.22 ± 2.93
	$\text{CH}_3\text{CH}_2\text{Y}(\text{C(O}\bullet)\text{OOCH}_2) \rightarrow \text{TS51}$ $\text{TS51} \rightarrow \text{CH}_3\text{CH}_2\text{C}(=\text{O})\text{O}\bullet + \text{CH}_2=\text{O}$ Average	-6.96 -7.50 -7.23 ± 0.38	-5.73 -8.64 -7.19 ± 2.06	- - -

ketene plus an ethyl radical. There are two keto-enol isomerization steps with barriers of 50.5 kcal mol⁻¹ (TS0) for hydrogen transfer from the secondary carbon group to form $\text{CH}_2\cdot\text{C}(\text{OH})=\text{CHCH}_3$ and 63.0 kcal mol⁻¹ (TS02a) for hydrogen transfer from the C-H₂ primary radical site to form $\text{CH}=\text{C}(\text{OH})\text{CH}_2\text{CH}_3$.

These two radicals can undergo beta scission/elimination of the hydroxyl group to form 1,2 butadiene with a barrier of 53.1 kcal mol⁻¹ (TS01) and 1-butyne with a barrier of 29.1 kcal mol⁻¹ (TS02), respectively. There is a high barrier (82.7 kcal mol⁻¹)

needed for the attack of the C-H₂ radical to the carbonyl oxygen (TS03) to form an epoxide in which the radical formed on the carbonyl carbon then undergoes beta scission to eliminate a methyl radical and from a methyleneoxirane. These barriers are relatively high for hydrocarbon radical elimination reactions, and sufficient temperature range is available to favor reactions with O₂.

4. Reaction of the 2-Butanone-1-yl Radical $\text{CH}_2\cdot\text{C}(=\text{O})\text{CH}_2\text{CH}_3 + \text{O}_2$. Figure 2 illustrates the major reaction paths in the $\text{CH}_2\cdot\text{C}(=\text{O})\text{CH}_2\text{CH}_3 + \text{O}_2$ reaction system. The association

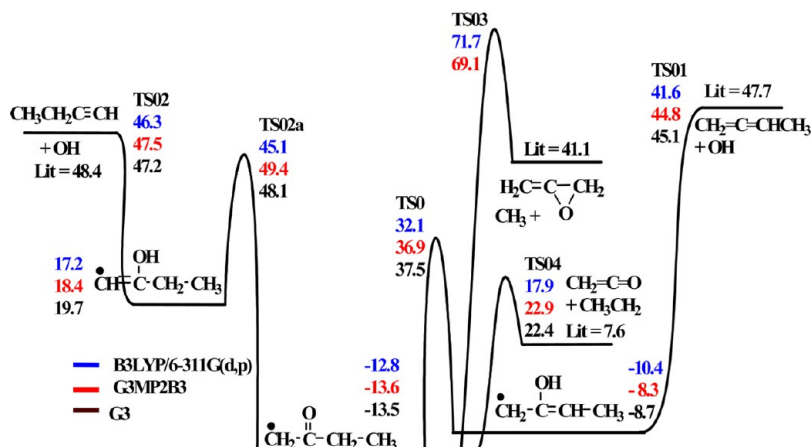


Figure 1. Potential energy curve for $\text{CH}_2\cdot\text{C}(=\text{O})\text{CH}_2\text{CH}_3$ to 1-butyne + OH, methylallene + OH, methyleneoxirane + CH_3 , and $\text{CH}_3\text{CH}_2 + \text{CH}_2=\text{C}=\text{O}$.

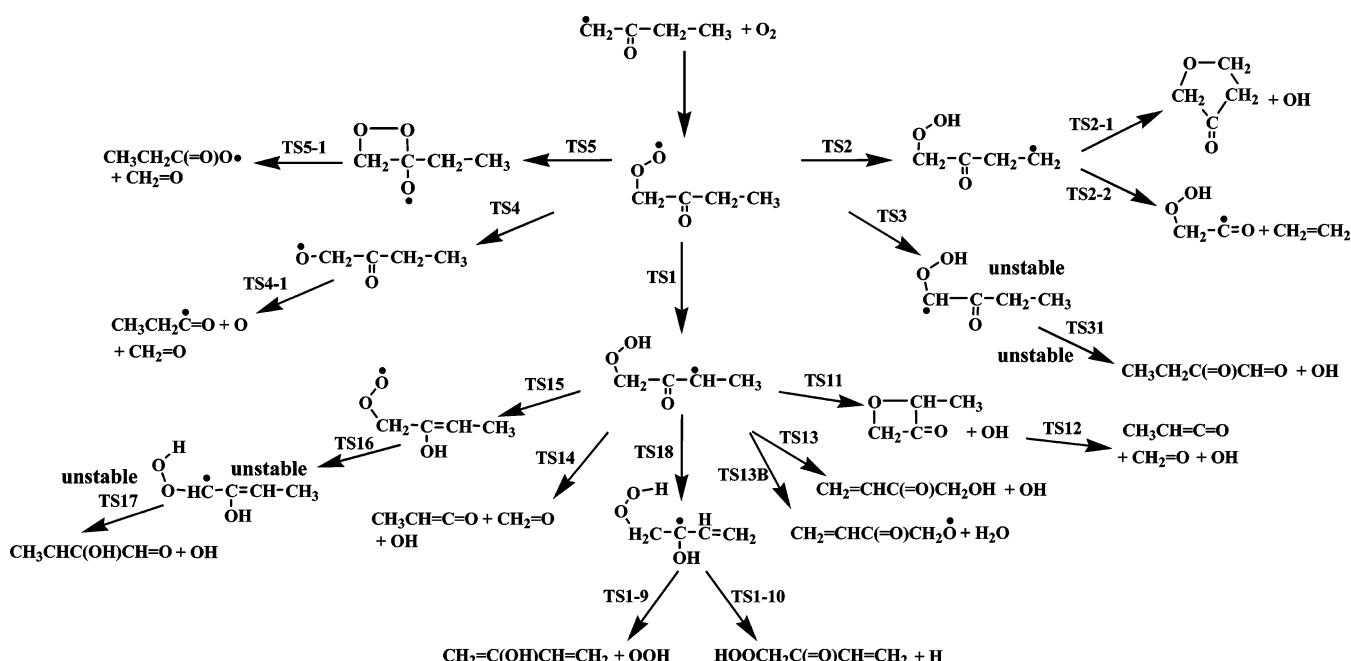


Figure 2. Major reaction channels for the $\text{CH}_2\cdot\text{C}(=\text{O})\text{CH}_2\text{CH}_3 + \text{O}_2$ reaction system.

results in a chemically activated peroxy radical $[\text{CH}_2\text{OO}\cdot\text{C}(=\text{O})\text{CH}_2\text{CH}_3]^{\#}$. Reactions available to this energized adduct include

- formation of a stable peroxy radical;
- reverse reaction back to 2-butanone-1-yl radical + O_2 (no reaction);
- intramolecular abstraction of H from the carbon (C-3) by the peroxy site (TS1);
- intramolecular abstraction of H from the carbon (C-4) by the peroxy site (TS2);
- intramolecular abstraction of H from the carbon (C-1) by the peroxy site (TS3);
- RO-O bond cleavage (important only at very high temperature) (TS4); and
- peroxy radical addition at the carbonyl carbon, forming a cyclic peroxide ring (TS5).

4.1. Formation of the Peroxy Radical and $[\text{CH}_2\text{OO}\cdot\text{C}(=\text{O})\text{CH}_2\text{CH}_3]^{\#}$ Potential Surface. The stabilized peroxy radical is an important product at lower temperatures and at moderate to higher temperature combustion conditions. The saddle point for

the association reaction of the 2-butanone-1-yl radical with O_2 in the formation of the activated $[\text{CH}_2\text{OO}\cdot\text{C}(=\text{O})\text{CH}_2\text{CH}_3]^{\#}$ is determined by calculating a potential surface. The energy surface was calculated for dissociation of $\text{CH}_2(\text{OO}\cdot)\text{C}(=\text{O})\text{CH}_2\text{CH}_3$ to $\text{CH}_2\cdot\text{C}(=\text{O})\text{CH}_2\text{CH}_3 + \text{O}_2$ from optimized structures of $\text{CH}_2(\text{OO}\cdot)\text{C}(=\text{O})\text{CH}_2\text{CH}_3$ at C–O distances at the UB3LYP/6-311G(d,p) level by increasing the C–O distance by 0.01 and 0.1 Å from 1.4 to ~4 Å.

The results illustrated in Figure 3 show a small barrier (saddle point) of ~0.9 kcal mol⁻¹, which is in agreement with the results reported by Kuwata et al.⁵⁴ for a similar acetone $\text{CH}_3\text{C}(=\text{O})\text{CH}_2 + \text{O}_2$ system. In our previous study on the secondary radical site of 2-butanone ($\text{CH}_3\text{C}(=\text{O})\text{CH}\cdot\text{CH}_3$) association with O_2 ,¹⁴ no barrier and relatively loose variational transition state structures for the formation of the activated peroxy intermediate^{55,56} were reported. One possible reason for the lack of the small barrier in the secondary system is the difference in bonding of the primary vs secondary carbon radical and oxy systems with the carbonyl group. There is a significant difference

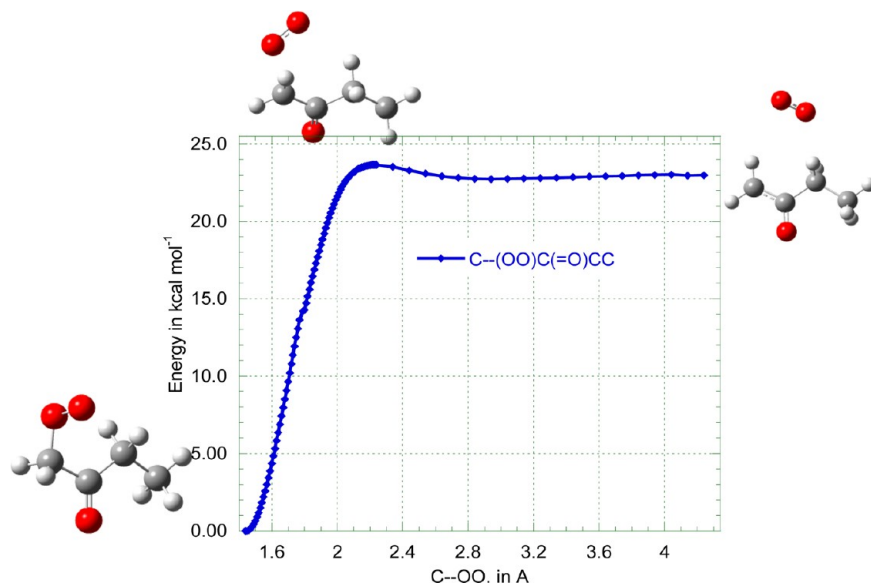


Figure 3. Dissociation of $\text{CH}_2(\text{OO}\cdot)\text{C}(=\text{O})\text{CH}_2\text{CH}_3$ to $\text{CH}_2\cdot\text{C}(=\text{O})\text{CH}_2\text{CH}_3 + \text{O}_2$.

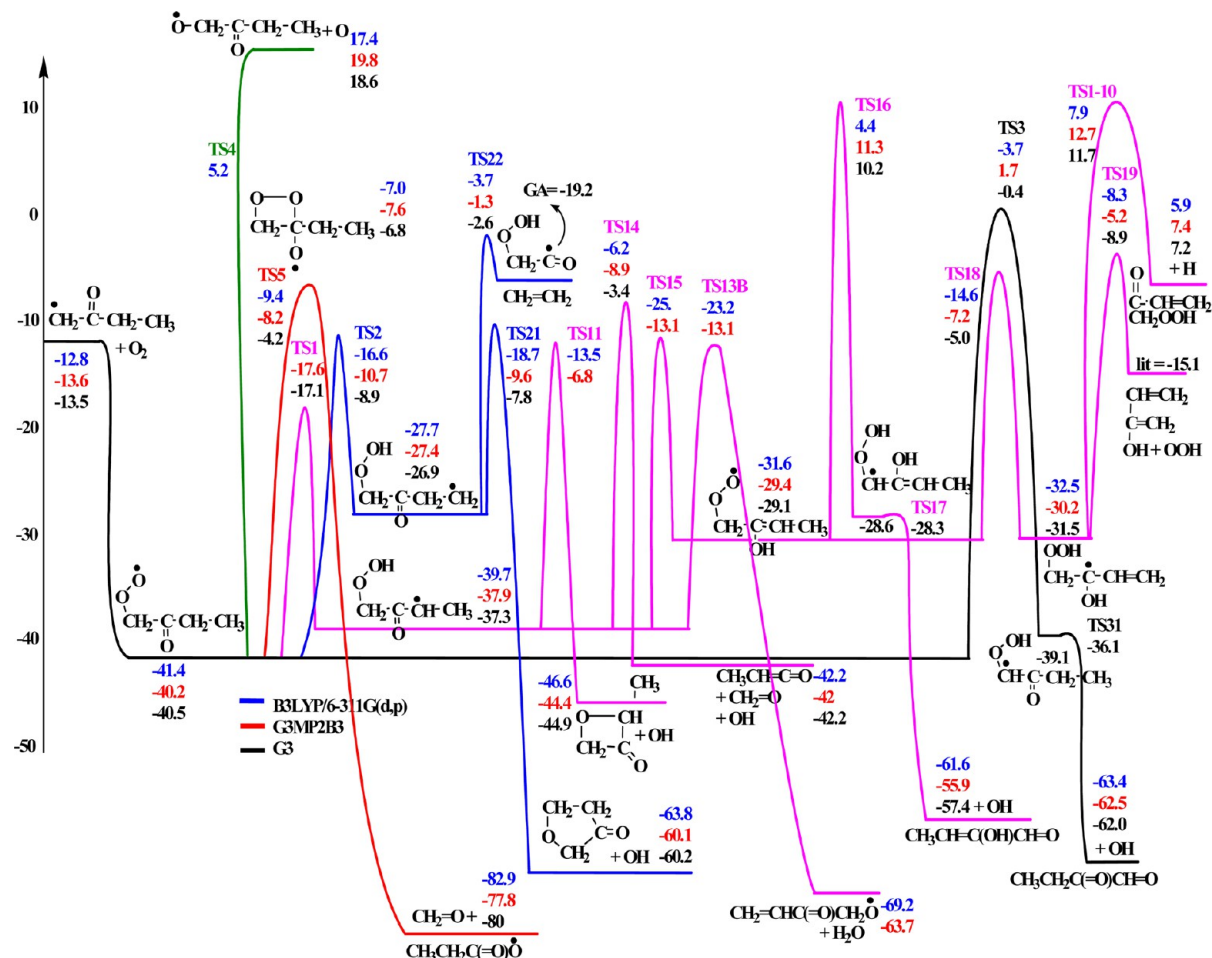


Figure 4. The $\text{CH}_2\cdot\text{C}(=\text{O})\text{CH}_2\text{CH}_3 + \text{O}_2$ system.

in the primary and secondary C–H bond energies on 2-butanone; the secondary C–H bond energy ($\text{CH}_3\text{C}(=\text{O})\text{CH}(-\text{H})\text{CH}_3$) is lower by 5 kcal mol⁻¹ than the primary C–H bond ($(\text{H}-)\text{CH}_2\text{C}(=\text{O})\text{CH}_2\text{CH}_3$, 95 kcal mol⁻¹) adjacent to the carbonyl in butanone at and in acetone.

The $\text{R}\cdot + \text{O}_2$ well depths are, however, similar in both the primary and secondary radicals ($\text{CH}_3\text{C}(=\text{O})\text{CHOO}\cdot\text{CH}_3$ and $\text{CH}_2\text{OO}\cdot\text{C}(=\text{O})\text{CH}_2\text{CH}_3$ at 26 and 27 kcal mol⁻¹ (G3 calculation level at 298 K)) and in the acetone systems. The shallow well is a result of loss of resonance between the

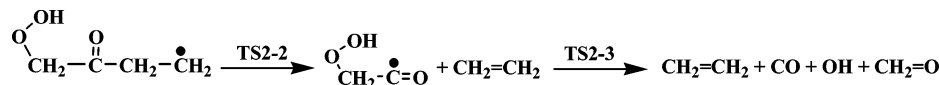


Figure 5. Dissociation reactions of $\text{CH}_2(\text{OOH})\text{C}(=\text{O})\text{CH}_2\text{CH}_2\cdot$ through TS2-2 and TS2-3.

carbon radical and the carbonyl group in formation of the new R—OO bond.

A detailed description of these reaction paths is given in the following sections. The transition state structures of the continuing reactions from each of these primary paths are numbered according to the respective initial path TS1-1, TS1-2, ... for TS1, TS2-1 for TS2 etc., as illustrated in Table 3 and Figures 4 and 5.

Figure 4 shows the potential surface and the reactions available to the chemically activated adduct $[\text{CH}_2\text{OO}\cdot\text{C}(=\text{O})\text{CH}_2\text{CH}_3]^{\#}$. The following sections discuss the individual reaction paths for this activated and stabilized-peroxy radical adduct.

4.2. Intramolecular Hydrogen Abstraction from Secondary Carbon C-3 (TS1). The peroxy oxygen radical site can abstract a hydrogen atom from the secondary carbon (C-3) adjacent to the carbonyl group over a barrier of 23 kcal mol⁻¹ (TS1), relative to the stabilized peroxide and 4 kcal mol⁻¹ below the entrance channel. This is the lowest barrier-forward channel. The low barrier is explained by the relatively weak C—H bond energy (~ 90 kcal mol⁻¹), which is the lowest on this $\text{CH}_2\text{OO}\cdot\text{C}(=\text{O})\text{CH}_2\text{CH}_3$ radical¹⁴ combined with a six-member cyclic transition state structure that has little ring strain. The radical formed, $\text{CH}_2\text{OOHC(=O)CH}\cdot\text{CH}_3$, is the lowest-energy peroxide intermediate, at -38 kcal mol⁻¹.

The newly formed secondary hydroperoxide alkyl radical $\text{CH}_2\text{OOHC(=O)CH}\cdot\text{CH}_3$ is shown to further react to five different product sets:

1. The low barrier path has the alkyl radical insert (bond) to the peroxide oxygen on the carbon, forming a four-member cyclic ether (lactone in this case) with elimination of OH (TS1-1). This is the stable 3-oxetanone, 4-methyl ($\text{O}=\text{Y}-(\text{CCH}_2\text{OCH})\text{CH}_3$) at -31 kcal mol⁻¹ on the PE surface. The energy needed for this OH elimination is similar to that of the entrance channel. At high temperature combustion conditions, this stable lactone may undergo dissociation through ring-opening to form aldehyde and methyl ketene over a 49 kcal mol⁻¹ barrier (TS1-2 in Table 3).

2. The second path for this $\text{CH}_2\text{OOHC(=O)CH}\cdot\text{CH}_3$ radical is complex, involving several atom movements; it is further illustrated later in the manuscript. In brief, the radical site is undergoing beta scission of a H atom on the C4 methyl. This leaving H atom is attacking the peroxy group oxygen that is bonded to the carbon, and the OH of the peroxide is cleaved. This reaction has a 53 kcal mol⁻¹ barrier (TS1-3) to form a stable, vinyl ketone-alcohol $\text{CH}_2=\text{CHC(=O)CH}_2\text{OH} + \text{OH}$.

3. Somewhat similar to TS1-3, the C4 H atom shifts to OH of the peroxide resulting in H_2O elimination and $\text{CH}_2(\text{O}\cdot)\text{C}(=\text{O})\text{CH}=\text{CH}_2$ (TS1-3B) with an only -13.3 kcal mol⁻¹ energy barrier. A similar H_2O elimination has also been recently identified⁵⁷ in peroxide alcohols. In our kinetic calculations, we consider TS1-3B.

4. Formation of ketene, formaldehyde, and OH (TS1-4) starts with a beta scission elimination through a barrier of 29 kcal mol⁻¹. The ketene ($\text{CH}_3\text{CH}=\text{C=O}$) is formed plus the hydroperoxide methyl radical ($\text{C}\cdot\text{H}_2\text{OOH}$), which immediately dissociates to $\text{CH}_2=\text{O} + \text{OH}$ via cleavage of the weak

C— H_2O —OH bond and formation of a strong π carbonyl bond (~80 kcal mol⁻¹).

5. The fifth path for $\text{CH}_2\text{OOHC(=O)CH}\cdot\text{CH}_3$ consists of the hydrogen attack on the carbonyl group forming $\text{CH}_2(\text{OO}\cdot)\text{C}(\text{OH})=\text{CHCH}_3$ through a barrier of 25 kcal mol⁻¹ (TS1-5) at -29 kcal mol⁻¹. The newly formed peroxy radical may undergo two H-shift reactions: (i) at the ipso position (from C1, TS1-6) to form $\text{CH}_3\text{CH}=\text{C}(\text{OH})\text{CH}=\text{O} + \text{OH}$ or (ii) from C2 (TS1-8) to form $\text{CH}_2(\text{OOH})\text{C}(\text{OH})\text{CH}=\text{CH}_3$, which can eliminate OOH (TS1-9) or a H atom (TS1-10), but this H elimination has a higher barrier.

4.3. Intramolecular Hydrogen Transfer from the Primary Carbon C-4 (TS2). A primary alkyl radical hydroperoxide, $\text{CH}_2(\text{OOH})\text{C}(=\text{O})\text{CH}_2\text{CH}_2\cdot$, is formed via an intramolecular hydrogen atom transfer from the C-4 primary carbon to the peroxy oxygen over a 31 kcal mol⁻¹ barrier (TS2) relative to the stabilized peroxy radical; this abstraction path is ~3 kcal mol⁻¹ above the entrance channel. The high barrier is a result of the strong primary C—H bond of ~100 kcal mol⁻¹.

The lowest forward barrier for this primary alkyl radical is attack (insertion) into the peroxy oxygen on the carbon, forming a cyclic ether (lactone) and eliminating OH radical from the peroxide. Formation of this lactone has a relatively low barrier of 18 kcal mol⁻¹ (TS2-1) relative to $\text{CH}_2(\text{OOH})\text{C}(=\text{O})\text{CH}_2\text{CH}_2\cdot$, and the overall reaction is exothermic with 33 kcal mol⁻¹ to the stable lactone at -69 kcal mol⁻¹. The reverse reactions of this primary radical—back to the peroxy radical and reaction to the lactone plus OH—have identical barriers; both are 5–6 kcal mol⁻¹ above the entrance channel.

This hydroperoxide alkyl radical can also undergo a beta scission reaction to form $\text{CH}_2=\text{CH}_2 + (\text{HOO})\text{CH}_2\text{C}=\text{O}$ (TS2-2) through a higher barrier of 26 kcal mol⁻¹. The $(\text{HOO})\text{CH}_2\text{C}=\text{O}$ formed will further decompose to $\text{CO} + \text{OH} + \text{CH}_2=\text{O}$ (TS2-3; see Table 3 and Figure 5).

4.4. Ipso Intramolecular Hydrogen Abstraction from Peroxy Radical Carbon C-1 (TS3). The peroxy oxygen radical abstracts a H atom from the same primary carbon (C-1), adjacent to the carbonyl group. Reaction occurs via a strained four-member-ring transition state structure and has a barrier of 41 kcal mol⁻¹ (TS3) relative to the peroxy radical; this is 14 kcal mol⁻¹ higher than the entrance channel. The reaction forms an unstable intermediate, $\text{CH}\cdot(\text{OOH})\text{C}(=\text{O})\text{CH}_2\text{CH}_3$, at -39 kcal mol⁻¹ (G3 level). The weak RC—O—OH bond cleaves immediately via electron rearrangement, forming the stable 2-butanone-2al $\text{CH}_3\text{CH}_2\text{C}(=\text{O})\text{CH}=\text{O}$ plus OH radical at -62 kcal mol⁻¹. The overall reaction is exothermic and releases some 22 kcal mol⁻¹ relative to the stable peroxy. The high barrier for the H transfer step and shallow chemical activation limit the importance of this reaction path at low temperature, but the importance increases at higher temperatures.

4.5. Simple Dissociation of the RO—O Bond of the Peroxide Radical (TS4). Figure 4, showing the simple dissociation of the $\text{CH}_2(\text{OO}\cdot)\text{C}(=\text{O})\text{CH}_2\text{CH}_3$ radical to $\text{CH}_2\text{O}\cdot\text{C}(=\text{O})\text{CH}_2\text{CH}_3 + \text{O}$ has been estimated by calculating the structure and energy of $\text{CH}_2(\text{OO}\cdot)\text{C}(=\text{O})\text{CH}_2\text{CH}_3$ against the CO—O distance for variational transition state analysis. The unrestricted DFT calculations did not show a saddle point (TS4) for this system.

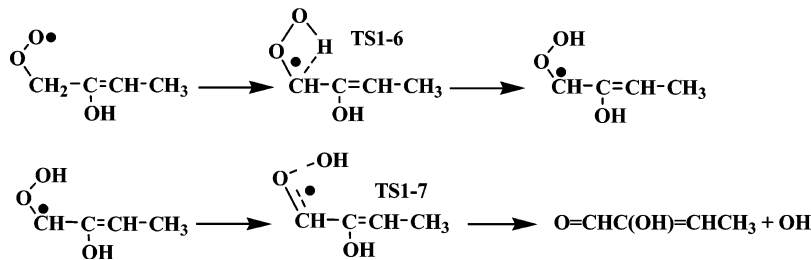


Figure 6. Two-step transition state structure calculation with G3 method.

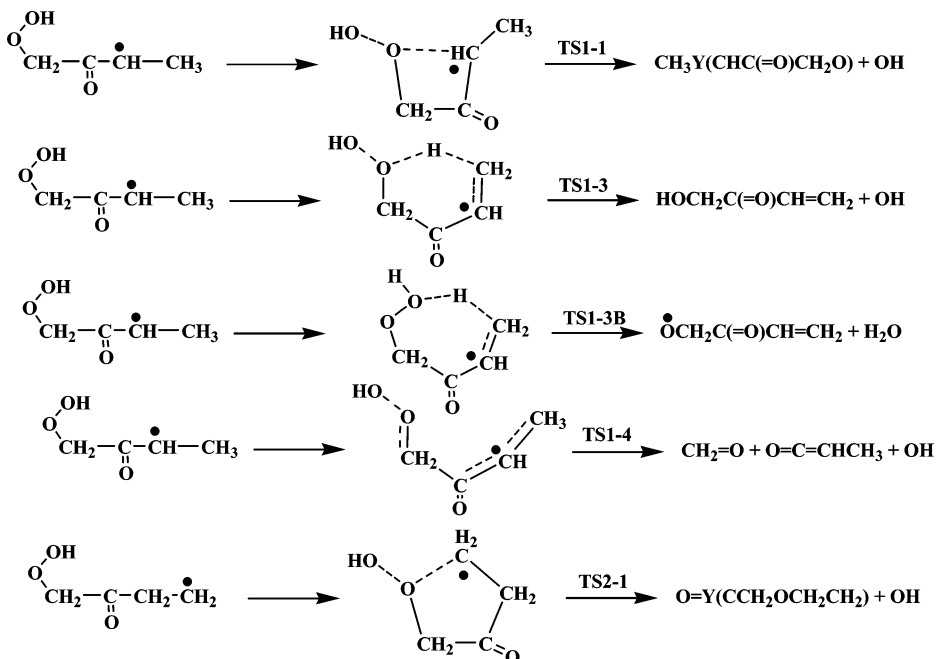


Figure 7. Transition state structures calculation with the G3MP2B3 method.

This is similar to the results obtained on benzoyl and phenyl systems.^{58,42,55,56} The endothermicity of the reaction, 46 kcal mol⁻¹, is similar to phenyl and vinyl-peroxy systems, but ~14 kcal mol⁻¹ lower than primary, secondary, and tertiary alkyl radicals. The 14 kcal mol⁻¹ reflects the stabilization of the CH₂(O·)C(=O)CH₂CH₃ moiety and that the resonance stabilization is similar to phenyl-O and vinyl-O interactions. We further note that this C(O—O)C(=O)CC dissociation is some 8 kcal mol⁻¹ lower than that required for the 2-butanone-3yl, for which the dissociation energy barrier was found to be 54 kcal mol⁻¹.¹⁴

The relatively unstable CH₂(O·)C(=O)CH₂CH₃ radical dissociates without a barrier (TS4-1; see Table 3) to form an aldehyde plus a propanoyl radical (CH₂=O + CH₃CH₂C·=O). The high RO—O dissociation barrier, 15 kcal mol⁻¹ above the entrance channel, limits the importance of this channel to some extent, but it may have importance at high temperatures because it is a chain branching reaction.

4.6. Addition of the Peroxy-Oxygen Radical to the Carbonyl Group Carbon C-2 (TS5). A reaction involving the peroxy radical site attack on the carbonyl carbon, opening the double bond on the carbon of the carbonyl group, is generally not considered in the peroxy chemistry because it has to open the strong (~80 kcal mol⁻¹) carbonyl Π bond. It forms a reactive cyclic peroxide alkoxy radical (CH₃CH₂Y(C(O·)OOCH₂; see Figure 4 and Table 2). This interesting addition to the carbonyl has a

barrier of 32 kcal mol⁻¹ (TSS), relative to the peroxy radical, with tight transition state at 4 kcal mol⁻¹ above the entrance channel. When formed, the cyclic peroxide alkoxy radical dissociates without barrier (TS5-1; see Table 3) to CH₂=O plus a propanoyl radical (CH₃CH₂C(=O)O·) with a release of 70 kcal mol⁻¹.

5. Selected Transition State Structures and Differences Resulting from Calculation Method. 5.1. *Ipsò Abstraction.*

Ipsò abstraction occurs when the peroxy radical abstracts a hydrogen atom from the same carbon to which the peroxy radical is bonded. The type of overall reaction can occur as a sequential two-step or as a single-step process. In this (and other similar peroxy systems), we find that the G3 method with the MP2 calculation treats it as sequential, whereas the B3LYP/6-311G(d,p) and the G3MP2B3 calculate it as a single step. In the MP2 sequential calculation, the peroxy radical abstracts the H atom, forming a hydroperoxide with a radical on the peroxide carbon (see Figure 6). The MP2 then sees a small barrier to beta scission reaction, forming a new carbonyl bond and cleaving the OH radical. The DFT calculations in the B3LYP and G3MP2B3 do not “see” the second barrier for the beta scission process, but have the reaction as concerted.

In the thermochemistry of the abstraction, the first step in G3 is 1 kcal mol⁻¹ endothermic in the G3 calculation, and the barrier for the abstraction is 40 kcal mol⁻¹ from a combination of a slightly endothermic abstraction and strain in the 4-member ring

Table 4. Input Parameters^a and High-Pressure Limit Rate Constants (k_{∞}) for QRRK Calculations

reaction	A	n	k_{∞}
			E_a (kcal mol ⁻¹)
$\text{CH}_2\cdot\text{C}(=\text{O})\text{CH}_2\text{CH}_3 + \text{O}_2 \rightarrow \text{CH}_2\text{OO}\cdot\text{C}(=\text{O})\text{CH}_2\text{CH}_3$	3.00×10^{12}	0	0
$\text{CH}_2\text{OO}\cdot\text{C}(=\text{O})\text{CH}_2\text{CH}_3 \rightarrow \text{CH}_2\cdot\text{C}(=\text{O})\text{CH}_2\text{CH}_3 + \text{O}_2$	9.7802×10^{14}	0.065437	35.1
$\text{CH}_2\text{OO}\cdot\text{C}(=\text{O})\text{CH}_2\text{CH}_3 \rightarrow \text{CH}_2(\text{OOH})\text{C}(=\text{O})\text{CH}_2\text{CH}_3$	1.5211×10^{15}	-2.87864	24.7
$\text{CH}_2\text{OO}\cdot\text{C}(=\text{O})\text{CH}_2\text{CH}_3 \rightarrow \text{CH}_2(\text{OOH})\text{C}(=\text{O})\text{CH}_2\text{CH}_2\cdot$	8.27×10^{14}	-2.84812	31.57
$\text{CH}_2\text{OO}\cdot\text{C}(=\text{O})\text{CH}_2\text{CH}_3 \rightarrow \text{CH}_3\text{CH}_2\text{C}(=\text{O})\text{CH}=\text{O} + \text{OH}$	8.25×10^{17}	-3.57748	44.55
$\text{CH}_2\text{OO}\cdot\text{C}(=\text{O})\text{CH}_2\text{CH}_3 \rightarrow \text{CH}_2(\text{O}\cdot)\text{C}(=\text{O})\text{CH}_2\text{CH}_3 + \text{O}$	9.42×10^{16}	-2.96554	47.78
$\text{CH}_2\text{OO}\cdot\text{C}(=\text{O})\text{CH}_2\text{CH}_3 \rightarrow \text{CH}_3\text{CH}_2\text{C}(=\text{O})\text{O}\cdot + \text{CH}_2=\text{O}$	1.34×10^{16}	-3.34482	34.46
$\text{CH}_2(\text{OOH})\text{C}(=\text{O})\text{CH}_2\text{CH}_3 \rightarrow \text{CH}_2\text{OO}\cdot\text{C}(=\text{O})\text{CH}_2\text{CH}_3$	7.75×10^7	0.75003	19.27
$\text{CH}_2(\text{OOH})\text{C}(=\text{O})\text{CH}_2\text{CH}_3 \rightarrow \text{CH}_3\text{Y}(\text{CHOCH}_2\text{C})=\text{O} + \text{OH}$	2.14×10^9	0.7575	30.39
$\text{CH}_2(\text{OOH})\text{C}(=\text{O})\text{CH}_2\text{CH}_3 \rightarrow \text{CH}_2(\text{O}\cdot)\text{C}(=\text{O})\text{CH}=\text{CH}_2 + \text{H}_2\text{O}$	1.56×10^6	1.34487	23.6
$\text{CH}_2(\text{OOH})\text{C}(=\text{O})\text{CH}_2\text{CH}_3 \rightarrow \text{CH}_3\text{CH}=\text{C}=\text{O} + \text{CH}_2=\text{O} + \text{OH}$	1.40×10^8	1.23011	28.11
$\text{CH}_2(\text{OOH})\text{C}(=\text{O})\text{CH}_2\text{CH}_3 \rightarrow \text{CH}_2(\text{OO}\cdot)\text{C}(\text{OH})=\text{CHCH}_3$	1.11×10^9	0.70604	23.79
$\text{CH}_2(\text{OO}\cdot)\text{C}(\text{OH})=\text{CHCH}_3 \rightarrow \text{CH}_2(\text{OOH})\text{C}(=\text{O})\text{CH}_2\text{CH}_3$	2.82×10^9	0.70772	15.85
$\text{CH}_2(\text{OO}\cdot)\text{C}(\text{OH})=\text{CHCH}_3 \rightarrow \text{CH}_3\text{CH}=\text{C}(\text{OH})\text{CH}=\text{O} + \text{OH}$	1.83×10^{11}	0.6899	40.58
$\text{CH}_2(\text{OO}\cdot)\text{C}(\text{OH})=\text{CHCH}_3 \rightarrow \text{CH}_2(\text{OOH})\text{C}(\text{OH})\text{CH}=\text{CH}_2$	9.21×10^7	0.96123	21.64
$\text{CH}_2(\text{OOH})\text{C}(=\text{O})\text{CH}_2\text{CH}_2\cdot \rightarrow \text{CH}_2\text{OO}\cdot\text{C}(=\text{O})\text{CH}_2\text{CH}_3$	3.17×10^8	0.56973	15.88
$\text{CH}_2(\text{OOH})\text{C}(=\text{O})\text{CH}_2\text{CH}_2\cdot \rightarrow \text{O}=\text{Y}(\text{CCH}_2\text{OCH}_2\text{CH}_2) + \text{OH}$	9.22×10^{12}	-0.0802	17.72
$\text{CH}_2(\text{OOH})\text{C}(=\text{O})\text{CH}_2\text{CH}_2\cdot \rightarrow \text{CH}_2(\text{OOH})\text{C}=\text{O} + \text{CH}_2=\text{CH}_2$	2.41×10^{10}	0.70894	25.52

^aThe units of A factors and rate constants, k , are s⁻¹ for unimolecular reactions and cm³ mol⁻¹ s⁻¹ for bimolecular reactions. All parameters A , n , and E_a , are fit over the temperature range of 500–2400 K.

transition state structure. In the second step, the beta scission process, a weak RC-O-OH peroxide bond is cleaved, and a carbonyl π bond is formed. In a nonradical, a generic RCO-OH peroxide bond dissociation energy is ~46 kcal mol⁻¹, and in a π carbonyl, RC=O adds 80 kcal mol⁻¹ to the RC-O σ bond. Cleaving a 45 kcal mol⁻¹ RO-OH bond and forming an 80 kcal mol⁻¹ bond is 35 kcal exothermic.

5.2. OH Elimination in TS1-4, TS1-1 and TS2-1. In Figure 7, the reaction for TS1-4 starts from the $\text{CH}_2\text{OOHC}(=\text{O})\text{CH}_2\text{CH}_3$ radical. The illustrated TS1-4 reaction is a beta scission in which a new double bond is being formed between C-3 and the carbonyl carbon, C-2. The formation of the new bond to C2 consumes one electron from the C1—C2 bond and cleaves the C1—C2 bond, forming $\text{C}_2\text{H}_2\text{OOH}$. Similar to the ipso systems above, the carbon radical in this intermediate forms a strong π bond with the oxygen and cleaves the weaker RO-OH bond. The $\text{CH}_2=\text{O} + \text{OH}$ products are formed.

TS1-1 and TS2-1 initiate from the $\text{CH}_2\text{OOHC}(=\text{O})\text{CH}_2\text{CH}_3$ and $\text{CH}_2\text{OOHC}(=\text{O})\text{CH}_2\text{CH}_3\cdot$ alkyl radicals, respectively. In the reactions illustrated by the equations in Figure 7, the alkyl radical is attacking the oxygen of the peroxide, which is bonded to the carbon. This S_N2 reaction forms a cyclic ether and as the carbon—oxygen ether bond is formed and the weaker RO-OH bond is cleaved, a cyclic ether is formed and an OH radical is eliminated. Further reactions of these cyclic ethers need to be considered in combustion mechanisms.

5.3. OH/H₂O Elimination in TS1-3 and TS1-3B. Two new (previously unreported) and important reactions to peroxide chemistry are presented in reactions TS1-3 and TS1-3b. Both of these reactions start with the hydroperoxy-3yl radical $\text{CH}_2(\text{OOH})\text{C}(=\text{O})\text{OC}\cdot\text{HCH}_3$. The molecule is in a near cyclic configuration, with a hydrogen from the C-4 methyl group undergoing H bonding to one of the oxygens in the peroxide. In both reactions, the C-3 carbon radical is in the beta scission structure initiating the formation of a double bond to C-4 and the elimination of a H atom from the C-4 methyl. The H atom being eliminated is H-bonding.

In reaction TS1-3B, the weak RO-OH bond is cleaved, leaving an alkoxy radical on carbon C1. The H atom being eliminated via beta scission (double bond formation of C3—C4) is H-bonding to the oxygen of the peroxide OH group. The H atom inserts into this O atom, forming and eliminating H_2O . The reaction barrier is low at ~15 kcal mol⁻¹, and this reaction will, in some reaction systems, have important implications for peroxy radical chemistry because the overall reaction is exothermic by 22 kcal mol⁻¹. It has some importance in this system but is limited by the shallow well depth and the barrier to form the $\text{CH}_2(\text{OOH})\text{C}(=\text{O})\text{C}\cdot\text{HCH}_3$ radical.

In reaction TS1-3, the H atom being eliminated via beta scission (double bond formation of C3—C4) is H-bonding to the first oxygen of the peroxide bonded to the carbon C-1. The H atom inserts into this O atom, forming an alcohol, and cleaves the weak RO-OH bond to form ROH + OH. The reaction barrier is high: near 50 kcal mol⁻¹.

6. Kinetic Calculations. Multichannel, multifrequency QRRK⁵⁹ calculations are performed for $k(E)$ with master equation analysis (CHEMASTER code) for falloff on the $\text{CH}_2\cdot\text{C}(=\text{O})\text{CH}_2\text{CH}_3 + \text{O}_2$ reaction systems to estimate rate constants and to determine important reaction paths as a function of temperature and pressure. The chemical activated peroxy radical intermediate [$\text{CH}_2\text{OO}\cdot\text{C}(=\text{O})\text{CH}_2\text{CH}_3$][#] is formed and can undergo isomerization or dissociation reactions, as illustrated in Figure 4, before stabilization by collisions. The calculations provide sets of rate constants, $k(T)$, for the formation of the stabilized adduct or new reaction products at different pressures. The bimolecular chemically activated kinetics use the barriers after the entrance channel, as illustrated in Figures 3 and 4. The QRRK with master equation analysis is also used for unimolecular dissociation of each adduct.

Pressure dependence is shown to be important in the kinetics of several product sets, and these may have importance in modeling different combustion and engine systems. Scram jet engines run at 0.3 atm, for example, whereas turbines run at pressure of 10–15 atm, internal combustion engines can

Table 5. Calculated Rate Constants with QRRK at $P = 1$ atm

reaction	calculated reaction parameters at $P = 1$ atm, $k = A(T/K)^n \exp(-E_a/RT)$		
	A	n	E_a (cal mol $^{-1}$)
$\text{CH}_2\cdot\text{C}(=\text{O})\text{CH}_2\text{CH}_3 + \text{O}_2 \rightleftharpoons \text{CH}_2\text{OO}\cdot\text{C}(=\text{O})\text{CH}_2\text{CH}_3$	$2.03 + 128$	-35.78	44183
$\text{CH}_2\cdot\text{C}(=\text{O})\text{CH}_2\text{CH}_3 + \text{O}_2 \rightleftharpoons \text{CH}_2\cdot\text{C}(=\text{O})\text{CH}_2\text{CH}_3 + \text{O}_2$	1.63×10^{30}	-4.87	14416
$\text{CH}_2\cdot\text{C}(=\text{O})\text{CH}_2\text{CH}_3 + \text{O}_2 \rightleftharpoons \text{CH}_3\text{CH}_2\text{C}(=\text{O})\text{CH}=\text{O} + \text{OH}$	2.93×10^{28}	-7.34	18128
$\text{CH}_2\cdot\text{C}(=\text{O})\text{CH}_2\text{CH}_3 + \text{O}_2 \rightleftharpoons \text{CH}_2(\text{O}\cdot)\text{C}(=\text{O})\text{CH}_2\text{CH}_3 + \text{O}$	9.65×10^{26}	-6.62	20242
$\text{CH}_2\cdot\text{C}(=\text{O})\text{CH}_2\text{CH}_3 + \text{O}_2 \rightleftharpoons \text{CH}_3\text{CH}_2\text{C}(=\text{O})\text{O} \cdot + \text{CH}_2=\text{O}$	5.66×10^{31}	-8.38	14250
$\text{CH}_2\cdot\text{C}(=\text{O})\text{CH}_2\text{CH}_3 + \text{O}_2 \rightleftharpoons \text{C}(\text{OOH})\text{C}(=\text{O})\text{CH}\cdot\text{CH}_3$	$1.25 + 156$	-45.65	62208
$\text{CH}_2\cdot\text{C}(=\text{O})\text{CH}_2\text{CH}_3 + \text{O}_2 \rightleftharpoons \text{CH}_3\text{Y}(\text{CHOCH}_2\text{C})=\text{O} + \text{OH}$	8.16×10^{54}	-14.45	33700
$\text{CH}_2\cdot\text{C}(=\text{O})\text{CH}_2\text{CH}_3 + \text{O}_2 \rightleftharpoons \text{CH}_2(\text{O}\cdot)\text{C}(=\text{O})\text{CH}=\text{CH}_2 + \text{H}_2\text{O}$	5.66×10^{57}	-15.42	33422
$\text{CH}_2\cdot\text{C}(=\text{O})\text{CH}_2\text{CH}_3 + \text{O}_2 \rightleftharpoons \text{CH}_3\text{CH}=\text{C}=\text{O} + \text{CH}_2=\text{O} + \text{OH}$	3.26×10^{55}	-14.44	33432
$\text{CH}_2\cdot\text{C}(=\text{O})\text{CH}_2\text{CH}_3 + \text{O}_2 \rightleftharpoons \text{CH}_2(\text{OOH})\text{C}(=\text{O})\text{CH}_2\text{CH}_2\cdot$	$2.02 + 131$	-39.66	46804
$\text{CH}_2\cdot\text{C}(=\text{O})\text{CH}_2\text{CH}_3 + \text{O}_2 \rightleftharpoons \text{O}=\text{Y}(\text{CCH}_2\text{OCH}_2\text{CH}_2) + \text{OH}$	3.82×10^{40}	-10.65	19583
$\text{CH}_2\cdot\text{C}(=\text{O})\text{CH}_2\text{CH}_3 + \text{O}_2 \rightleftharpoons \text{CH}_2(\text{OOH})\text{C}=\text{O} + \text{CH}_2=\text{CH}_2$	5.21×10^{30}	-7.93	20678
$\text{CH}_2\cdot\text{C}(=\text{O})\text{CH}_2\text{CH}_3 + \text{O}_2 \rightleftharpoons \text{CH}_2(\text{OO}\cdot)\text{C}(\text{OH})=\text{CHCH}_3$	$1.29 + 160$	-47.3	68428
$\text{CH}_2\cdot\text{C}(=\text{O})\text{CH}_2\text{CH}_3 + \text{O}_2 \rightleftharpoons \text{CH}_3\text{CH}=\text{C}(\text{OH})\text{CH}=\text{O} + \text{OH}$	2.67×10^{54}	-14.31	44721
$\text{CH}_2\cdot\text{C}(=\text{O})\text{CH}_2\text{CH}_3 + \text{O}_2 \rightleftharpoons \text{CH}_2(\text{OOH})\text{C}(\cdot\text{OH})\text{CH}=\text{CH}_2$	6.05×10^{62}	-16.92	40430
$\text{CH}_2\text{OO}\cdot\text{C}(=\text{O})\text{CH}_2\text{CH}_3 \rightleftharpoons \text{CH}_2\cdot\text{C}(=\text{O})\text{CH}_2\text{CH}_3 + \text{O}_2$	4.09×10^{62}	-14.89	51711
$\text{CH}_2\text{OO}\cdot\text{C}(=\text{O})\text{CH}_2\text{CH}_3 \rightleftharpoons \text{CH}_3\text{CH}_2\text{C}(=\text{O})\text{CH}=\text{O} + \text{OH}$	9.98×10^{73}	-21.58	61746
$\text{CH}_2\text{OO}\cdot\text{C}(=\text{O})\text{CH}_2\text{CH}_3 \rightleftharpoons \text{CH}_2(\text{O}\cdot)\text{C}(=\text{O})\text{CH}_2\text{CH}_3 + \text{O}$	1.27×10^{75}	-21.81	64569
$\text{CH}_2\text{OO}\cdot\text{C}(=\text{O})\text{CH}_2\text{CH}_3 \rightleftharpoons \text{CH}_3\text{CH}_2\text{C}(=\text{O})\text{O} \cdot + \text{CH}_2=\text{O}$	1.10×10^{63}	-18.06	50900
$\text{CH}_2\text{OO}\cdot\text{C}(=\text{O})\text{CH}_2\text{CH}_3 \rightleftharpoons \text{C}(\text{OOH})\text{C}(=\text{O})\text{CH}\cdot\text{CH}_3$	1.40×10^{50}	-13.69	37964
$\text{CH}_2\text{OO}\cdot\text{C}(=\text{O})\text{CH}_2\text{CH}_3 \rightleftharpoons \text{CH}_2(\text{OOH})\text{C}(=\text{O})\text{CH}_2\text{CH}_2\cdot$	2.87×10^{58}	-16.45	47229
$\text{CH}_2(\text{OOH})\text{C}(=\text{O})\text{CH}\cdot\text{CH}_3 \rightleftharpoons \text{CH}_3\text{Y}(\text{CHOCH}_2\text{C})=\text{O} + \text{OH}$	1.55×10^{44}	-9.94	44241
$\text{CH}_2(\text{OOH})\text{C}(=\text{O})\text{CH}\cdot\text{CH}_3 \rightleftharpoons \text{CH}_2=\text{CHC}(=\text{O})\text{CH}_2\text{OH} + \text{OH}$	2.05×10^{32}	-6.64	34118
$\text{CH}_2(\text{OOH})\text{C}(=\text{O})\text{CH}\cdot\text{CH}_3 \rightleftharpoons \text{CH}_3\text{CH}=\text{C}=\text{O} + \text{CH}_2=\text{O} + \text{OH}$	1.22×10^{40}	-8.55	40886
$\text{CH}_2(\text{OOH})\text{C}(=\text{O})\text{CH}\cdot\text{CH}_3 \rightleftharpoons \text{CH}_2(\text{OO}\cdot)\text{C}(=\text{O})\text{CH}_2\text{CH}_3$	1.15×10^{29}	-5.7	27980
$\text{CH}_2(\text{OOH})\text{C}(=\text{O})\text{CH}\cdot\text{CH}_3 \rightleftharpoons \text{CH}_2(\text{OO}\cdot)\text{C}(\text{OH})=\text{CHCH}_3$	2.18×10^{35}	-7.34	34356
$\text{CH}_2(\text{OOH})\text{C}(=\text{O})\text{CH}_2\text{CH}_2\cdot \rightleftharpoons \text{O}=\text{Y}(\text{CCH}_2\text{OCH}_2\text{CH}_2) + \text{OH}$	7.03×10^{32}	-6.56	23763
$\text{CH}_2(\text{OOH})\text{C}(=\text{O})\text{CH}_2\text{CH}_2\cdot \rightleftharpoons \text{CH}_2(\text{OOH})\text{C}=\text{O} + \text{CH}_2=\text{CH}_2$	6.94×10^{31}	-6.79	28495
$\text{CH}_2(\text{OOH})\text{C}(=\text{O})\text{CH}_2\text{CH}_2\cdot \rightleftharpoons \text{CH}_2\text{OO}\cdot\text{C}(=\text{O})\text{CH}_2\text{CH}_3$	3.56×10^{28}	-5.84	23080
$\text{CH}_2(\text{OO}\cdot)\text{C}(\text{OH})=\text{CHCH}_3 \rightleftharpoons \text{CH}_3\text{CH}=\text{C}(\text{OH})\text{CH}=\text{O} + \text{OH}$	6.87×10^{57}	14.84	51605
$\text{CH}_2(\text{OO}\cdot)\text{C}(\text{OH})=\text{CHCH}_3 \rightleftharpoons \text{CH}_2(\text{OOH})\text{C}(\cdot\text{OH})\text{CH}=\text{CH}_2$	2.68×10^{34}	-7.52	29802
$\text{CH}_2(\text{OO}\cdot)\text{C}(\text{OH})=\text{CHCH}_3 \rightleftharpoons \text{C}(\text{OOH})\text{C}(=\text{O})\text{CH}\cdot\text{CH}_3$	3.64×10^{31}	-6.21	24184

^aThe units of A factors and rate constants, k , are s^{-1} for unimolecular reactions and $\text{cm}^3 \text{mol}^{-1} \text{s}^{-1}$ for bimolecular reactions. All parameters, A , n , and E_a , are fit over the temperature range of 500–2400 K.

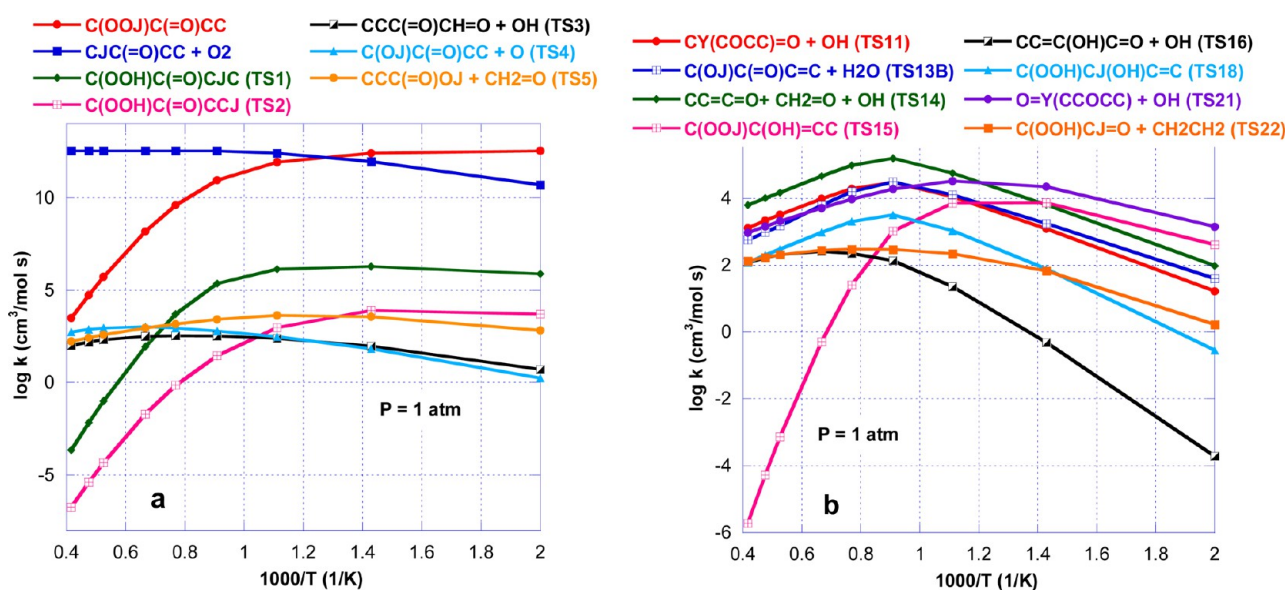


Figure 8. Calculated temperature-dependent rate constants for the chemically activated $\text{CH}_2\cdot\text{C}(=\text{O})\text{CH}_2\text{CH}_3 + \text{O}_2$ system at $P = 1$ atm. (Path b shows lower rate channels.)

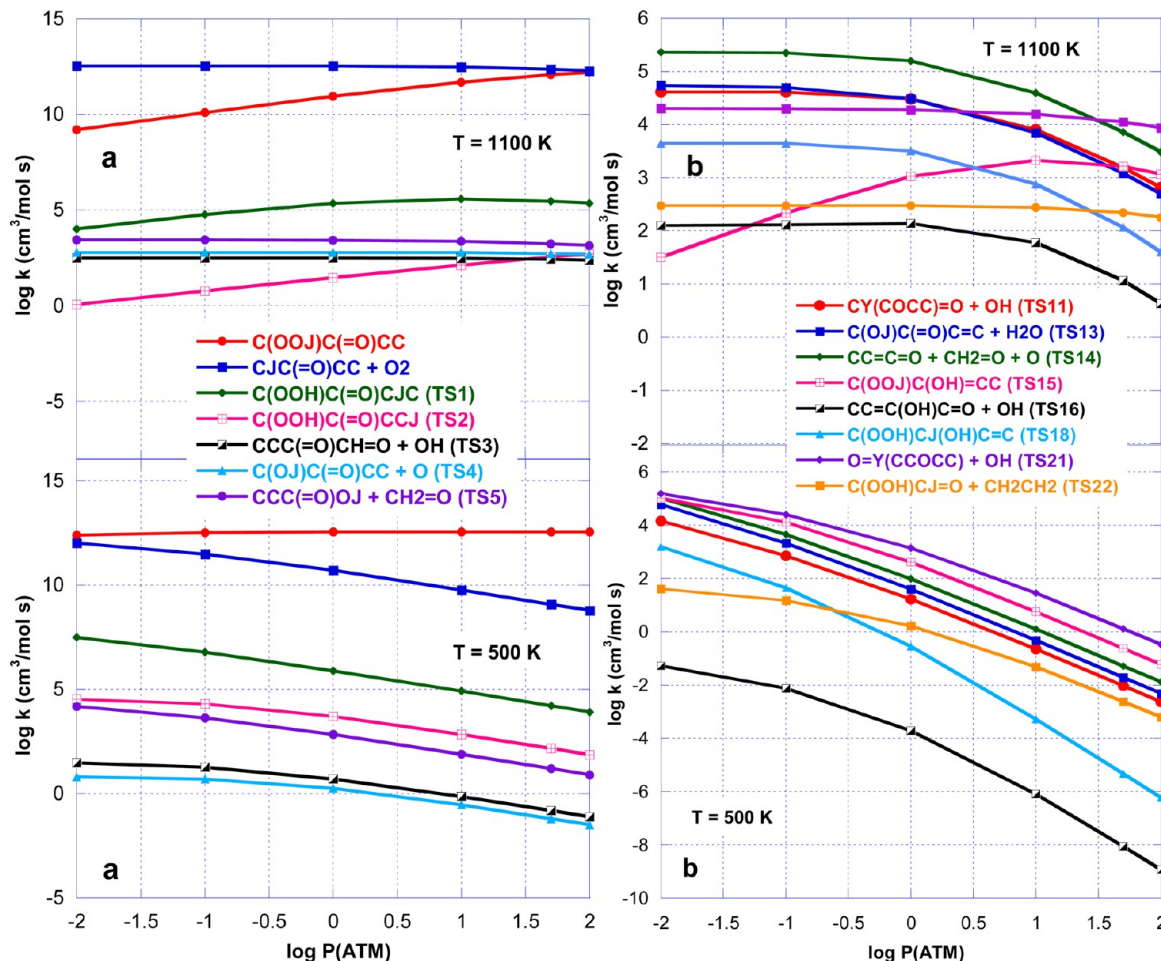


Figure 9. Calculated pressure-dependent rate constants for the chemically activated $\text{CH}_2\cdot\text{C}(=\text{O})\text{CH}_2\text{CH}_3 + \text{O}_2$ at $T = 500$ and 1100 K. (Path b shows lower rate channels.)

experience pressures to 100 atm, and higher pressures are being considered for improved efficiency.

Table 4 presents high-pressure-limit kinetic parameters for the reactions illustrated in Figure 4; these data are used as input data for the QRRK/Master Equation analysis code. Table 5 lists the reaction parameters at $P = 1$ atm for the temperature range of 500–2400 K. Reaction parameters at pressures ranging from 0.01 to 500 atm are listed in the Supporting Information.

The chemical activation reaction rate constants for the $\text{CH}_2\cdot\text{C}(=\text{O})\text{CH}_2\text{CH}_3 + \text{O}_2$ system are illustrated in Figure 8. There are seven product sets and several important intermediate isomers in this reaction system. The kinetics calculation results are listed in the figures with different scaled axes for clarity. The calculated temperature-dependent rate constants for the chemically activated $[\text{CH}_2\text{OO}\cdot\text{C}(=\text{O})\text{CH}_2\text{CH}_3]^{\#}$ reaction system from 500 to 2500 K at 1 atm are illustrated in Figure 8. Below 700 K (Figure 8a), the dominant product channel for this system is stabilization to the peroxy adduct $\text{CH}_2\text{OO}\cdot\text{C}(=\text{O})\text{CH}_2\text{CH}_3$. The reverse reaction from the chemically activated $[\text{CH}_2\text{OO}\cdot\text{C}(=\text{O})\text{CH}_2\text{CH}_3]^{\#}$, followed by the intramolecular H-abstraction reactions to form hydroperoxy-alkylradical isomers, is also important. One important H atom transfer occurs over (TS1) from the secondary carbon C-3, adjacent to the carbonyl group, to form $\text{CH}_2(\text{OOH})\text{C}(=\text{O})\text{CH}\cdot\text{CH}_3$. The abstraction from the primary carbon C-4 (TS2) to form $\text{CH}_2(\text{OOH})\text{C}(=\text{O})\text{CH}_2\text{CH}_2\cdot$ and addition to the carbonyl group (TS5) to form $\text{CH}_2=\text{O} + \text{CH}_3\text{CH}_2\text{C}(=\text{O})\text{O}\cdot$ are next in importance. The

barriers for RO-O cleavage and ipso H-abstraction from C_1 are too high, and these reactions are not important.

At higher temperatures, reverse reaction back to the 2-butanone-3yl radical plus O_2 is shown to be dominant because of the loose transition state structure. This is a nonreaction, and the $\text{CH}_2\cdot\text{C}(=\text{O})\text{CH}_2\text{CH}_3$ radical can continue to react. At temperatures above 1000 K, we note the strong falloff of the stabilized peroxy and the H transfer adducts from the secondary carbon C3 (TS1) and primary carbon C-4 (TS2). The O-O dissociation (TS4) of the stabilized peroxy radical as well as the 2-butanone-2-al plus OH radical channel (TS3) show some importance with increasing temperature.

The channels represented in Figure 8b are lower in importance than species represented in Figure 8a. At low temperature, the overall dominant channel is the formation of the lactone $\text{O}=\text{Y}(\text{CCH}_2\text{CH}_2\text{OCH}_2)$ (TS2-1), with the second lactone formation, $\text{CH}_3\text{Y}(\text{CHOCH}_2)=\text{O}$, via channel (TS1-1). The H_2O elimination (TS1-3B) and the dissociation reaction (TS1-4) are of importance, as well. We note also the falloff of the $\text{CH}_2(\text{OO}\cdot)\text{C}(\text{OH})=\text{CHCH}_3$ channel (TS1-5) above 900 K, whereas the $\text{CH}_3\text{CH}=\text{C}(\text{OH})\text{CH}=\text{O} + \text{OH}$ (TS1-6) and $\text{CH}_2(\text{OOH})\text{C}(\text{OH})\text{CH}=\text{CH}_2$ (TS1-8) product sets are formed through two channels, the most important being through the weakest H-abstraction from the primary carbon C4 (TS1-8).

At low temperature, ring closure to form $\text{O}=\text{Y}(\text{CCH}_2\text{CH}_2\text{OCH}_2) + \text{OH}$ (TS21) is favored, as shown in Figure 8b, but at high temperature, the dissociation reaction to

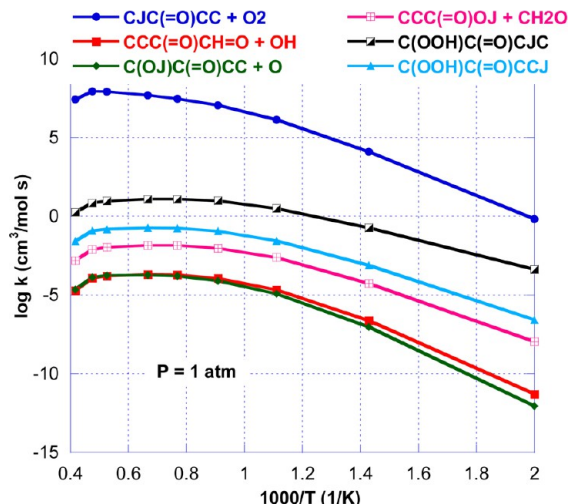


Figure 10. Calculated temperature-dependent rate constants for the dissociation reaction of $\text{CH}_2\text{OO}\cdot\text{C}(=\text{O})\text{CH}_2\text{CH}_3$ at $P = 1 \text{ atm}$.

$\text{CH}_3\text{CH}=\text{C}=\text{O} + \text{CH}_2=\text{O} + \text{OH}$ (TS14) shows dominance over the ring closure. The importance of the formation of the second lactone $\text{CH}_3\text{Y}(\text{CHOCH}_2\text{C})=\text{O}$ (TS11) increases with increasing temperature.

Figure 9a illustrates the pressure dependence for the rate constants of the chemically activated reaction systems at 500 and 1100 K. At both temperatures, dissociation back to the entrance channel reactants increases at lower pressures. Stabilization to the peroxy radical $\text{CH}_2\text{OO}\cdot\text{C}(=\text{O})\text{CH}_2\text{CH}_3$ with increasing pressure is the overall, dominant product channel, and it increases in importance at higher pressures. The intramolecular H-transfer from carbon C3 (TS1) is an important channel in this system at low and high temperature. At high temperature, it increases with pressure, whereas at the lower temperature, the increase in stabilization decreases the importance of this channel. The H-transfer to the peroxy site at the carbonyl carbon (TS2) is lower at 1100 K than at 500 K, and it increases with increasing pressure.

The next important reaction is peroxy addition on the carbonyl carbon, followed by the dissociation to $\text{CH}_2=\text{CH}_2$ and propanoic acid formation via (TS5); this channel decreases with pressure at 500 K and remains near constant over the pressure range at 1100 K. The remaining two channels,

describing the O–O dissociation (TS4) and the ipso intramolecular H-transfer to the peroxy oxygen (TS3) are of low importance at 500 K, and they also remain constant with pressure at 1100 K.

Figure 9b illustrates the further reactions of the primary product channels. The formation of lactone, $\text{O}=\text{Y}(\text{CCH}_2\text{CH}_2\text{OCH}_2) + \text{OH}$ (TS2-1), is dominant at low temperature, but at high temperature, the beta scission of the hydroperoxy-alkyl secondary radical channel (TS1-4) as well as the formation of the second lactone ($\text{CH}_3\text{Y}(\text{CHOCH}_2\text{C})=\text{O}$) over TS1-1 are more important. Formation of products decreases with increasing pressure at both temperatures as a result of stabilization of the initial adduct.

Figure 10 shows the unimolecular dissociation rate constants for the peroxy radical $\text{CH}_2(\text{OO}\cdot)\text{C}(=\text{O})\text{CH}_2\text{CH}_3$, and Figures 11a and b show the unimolecular dissociation of the two hydroperoxy-alkyl radicals, $\text{CH}_2(\text{OOH})\text{C}(=\text{O})\text{CH}\cdot\text{CH}_3$ and $\text{CH}_3(\text{OOH})\text{C}(=\text{O})\text{CH}_2\text{CH}_2\cdot$, as function of temperature at 1 atm. The dissociation of $\text{CH}_2(\text{OO}\cdot)\text{C}(=\text{O})\text{CH}_2\text{CH}_3$ (Figure 10) is dominated by the reaction back to the initial reactants, 2-butanone-1-yl + O_2 , followed in importance by the H-abstraction from the secondary carbon C3 to form a hydroperoxide ($\text{CH}_2(\text{OOH})\text{C}(=\text{O})\text{CH}\cdot\text{CH}_3$). The next two channels from the H-abstraction from the primary C4 and the addition (attack) of the peroxy site at the carbonyl carbon are lower in magnitude but still important.

The dissociation reactions of $\text{CH}_2(\text{OOH})\text{C}(=\text{O})\text{CH}\cdot\text{CH}_3$ (Figure 11a) show that the reverse reaction back to the peroxy radical is important for the dissociation of this adduct. The channel dominates at low temperatures, and it competes with a number of channels at the higher temperatures. One of the two new interesting channels, the H_2O elimination path is near an order of magnitude lower. This channel should become more important when the hydrogen transferring to the OH group is from a carbon site that is resonantly stabilized. The dissociation path to $\text{CH}_2=\text{CHC}(=\text{O})\text{CH}_2\text{OH} + \text{OH}$ is slow because of the higher barrier.

$\text{CH}_3(\text{OOH})\text{C}(=\text{O})\text{CH}_2\text{CH}_2\cdot$ dissociation (Figure 11b) shows three major paths, the lactone formation being markedly the most important, followed by reaction back to the peroxy radical $\text{CH}_2(\text{OO}\cdot)\text{C}(=\text{O})\text{CH}_2\text{CH}_3$. Elimination of ethylene is slightly slower.

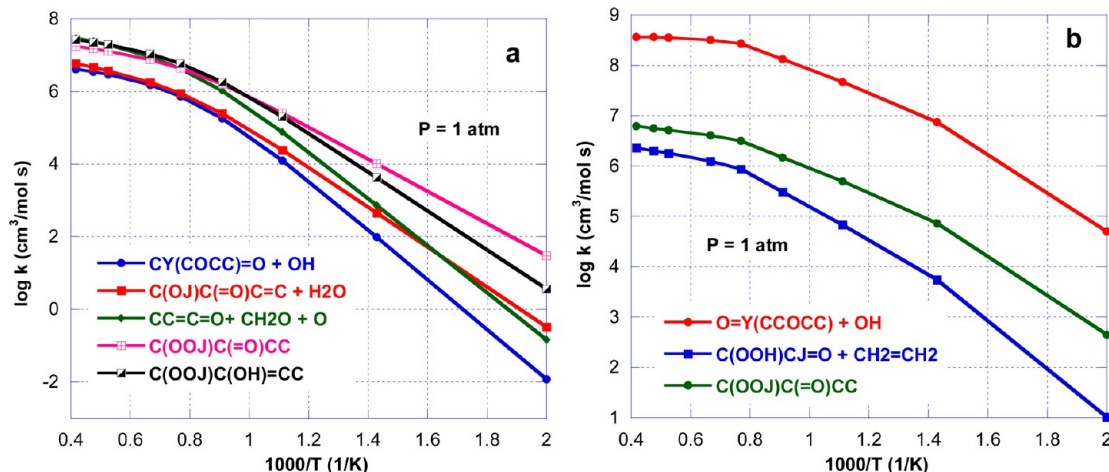


Figure 11. Calculated temperature-dependent rate constants for the dissociation reaction of (a) $\text{CH}_2(\text{OOH})\text{C}(=\text{O})\text{CH}\cdot\text{CH}_3$ and (b) $\text{CH}_2(\text{OOH})\text{C}(=\text{O})\text{CH}_2\text{CH}_2\cdot$ at $P = 1 \text{ atm}$.

Table 6

reactions	$\Delta_f H_{TS(298)}^0$ (kcal mol ⁻¹)				
radical → TS → products	B3LYP/6-311G(d,p)	G3MP2B3	G3MP2	G3	CBS-APNO
$\text{CH}_3\text{Y}(\text{CHC}(=\text{O})\text{CH}_2\text{O}) \rightarrow \text{TS1-2}$	-2.96	1.57	-4.88	-5.00	-4.38
$\text{TS1-2} \rightarrow \text{CH}_2=\text{O} + \text{CH}_3\text{CH}=\text{C=O}$	0.40	-7.47	-13.97	-14.4	-5.46
average					-4.92
$\text{TS1-2} \rightarrow \text{O}=\text{CHC}(=\text{O})\text{CH}_2\text{CH}_3$	-0.24	0.38	-5.63	-5.52	
$\text{CH}_2\cdot\text{C}(=\text{O})\text{CH}_2\text{CH}_3 \rightarrow \text{TS04}$	17.47	22.93	21.87	22.36	23.22
$\text{TS04} \rightarrow \text{CH}_2=\text{C=O} + \text{CH}_3\text{CH}_2$	18.26	14.41	13.51	13.67	13.57
average					18.39
$\text{TS04} + \text{H}_2 \rightarrow \text{CH}_2=\text{O} + \text{CH}_3\text{CH}_2\text{CH}_2$	13.77	22.12	21.12	22.02	

CONCLUSION

The 2-butanone-1-yl radical, $\text{CH}_2\cdot\text{C}(=\text{O})\text{CH}_2\text{CH}_3$ ($\Delta_f H_{298}^0 = 13.6$ kcal mol⁻¹ at G3MP2B3 calculation), reacts with O_2 to form a $\text{CH}_2\text{OO}\cdot\text{C}(=\text{O})\text{CH}_2\text{CH}_3$ radical with a 27 kcal mol⁻¹ well depth. Enthalpy, $\Delta_f H_{298}^0$, of important intermediates, transition state structures, and products resulting from this association were determined by using DFT (B3LYP/6-311G(d,p) level), ab initio (G3MP2B3 and G3), and group additivity. Isodesmic work reactions were used whenever possible to improve accuracy. Excellent agreement is obtained among the three methods for the radicals and stable species. The calculation reveals that DFT estimations are not accurate for several transition state structures. This result was noted in the previous investigated system, $(\text{CH}_3\text{C}(=\text{O})\text{CH}\cdot\text{CH}_3 + \text{O}_2)$.¹⁴

Reaction channels for the energized adduct $[\text{CH}_2(\text{OO}\cdot)\text{C}(=\text{O})\text{CH}_2\text{CH}_3]^{\#}$ include dissociation back to reactants; stabilization; intramolecular reactions by hydrogen transfer to the peroxy radical from three different carbon sites; ring closure reaction to $\text{CH}_3\text{Y}(\text{CHOCH}_2\text{C}(=\text{O}))$ and $\text{CH}_3\text{C}(=\text{O})\text{Y}(\text{CHOCH}_2)$; and dissociation to stable products and radicals $\text{CH}_3\text{CH}=\text{C=O}$, $\text{CH}_2=\text{O}$, $\text{CH}_3\text{CH}=\text{C(OH)CH=O}$, $\text{CH}_3\text{CH}_2\text{C}(=\text{O})\text{CH=O}$, $\text{CH}_2=\text{CHC}(=\text{O})\text{CH}_2\text{OH}$, $\text{CH}_2(\text{O}\cdot)\text{C}(=\text{O})\text{CH=CH}_2$, and $\text{CH}_3\text{CH}_2\text{C}(=\text{O})\text{O}^-$; and OH elimination. A new peroxy chemistry reaction path is presented. It has a low barrier path and involves a concerted reaction, resulting in olefin formation, H_2O elimination, and an alkoxy radical; it will have significant importance in alkyl peroxy radical systems.

APPENDIX

Three additional methods (CBS-APNO, M06-2X, and G3MP2) have been calculated for transition state structures TS1-2 and TS04 because of the significant differences in the different calculation methods used. In addition, work reactions that do not involve ketenes for TS04 and TS1-2 have been tried (see Table 6). These hypothetical reactions reproduce the values near -5 kcal mol⁻¹ for TS1-2 and 22.5 kcal mol⁻¹ for TS04, with G3, G3MP2, G2MP2, and CBS-APNO. We feel that the CBS-APNO method with the QCISD(T) calculation for the structure should be most accurate for a TS structure. The agreement among G3, G3MP2, and CBS-APNO for these transition state structures is now noted; the data are in Table 3. We recommend and have used the average from these three methods, -4.9 kcal mol⁻¹ for TS1-2 and the average of G3MP2B3, G3, and G3MP2, 22.5 kcal mol⁻¹, for TS04.

ASSOCIATED CONTENT

Supporting Information

SM1: Calculated thermochemical properties of radicals and stable species. SM2: Calculated thermochemical properties of transition state structures. SM 3: Geometry parameters for

radicals and transition state species. SM 4: Vibration frequencies^a (cm^{-1}) for radicals and transition state species. SM 5: Moment of inertia for radicals and transition state species. SM 6: Input file for QRRK with master code analysis (CHEMASTER). SM 7: CJCCDO.DAT file of NASA polynomials for use in CHEMKIN modeling. This information is available free of charge via the Internet at <http://pubs.acs.org>

AUTHOR INFORMATION

Corresponding Author

*E-mail: bozzelli@njit.edu.

Notes

The authors declare no competing financial interest.

REFERENCES

- Schulz, C.; Sick, V. Tracer-LIF Diagnostics: Quantitative Measurement of Fuel Concentration, Temperature and Fuel/Air Ratio in Practical Combustion Systems. *Prog. Energy Combust. Sci.* **2005**, *31*, 75–121.
- Hanson, R. K.; Seitzman, J. M.; Paul, P. H. Planar Laser-Fluorescence Imaging of Combustion Gases. *Appl. Phys. B: Laser Opt.* **1990**, *50*, 441–454.
- Pepiot-Desjardins, P.; Pitsch, H.; Malhotra, R.; Kirby, S. R.; Boehman, A. L. Structural Group Analysis for Soot Reduction Tendency of Oxygenated Fuels. *Combust. Flame* **2008**, *154*, 191–205.
- Hong, Z.; Davidson, D. F.; Vasu, S. S.; Hanson, R. K. The Effect of Oxygenates on Soot Formation in Rich Heptane Mixtures: A Shock Tube Study. *Fuel* **2009**, *88*, 1901–1906.
- Wolfe, G. M.; Crounse, J. D.; Parrish, J. D.; St. Clair, J. M.; Beaver, M. R.; Paulot, F.; Yoon, T. P.; Wennberg, P. O.; Keutsch, F. N. Photolysis, OH Reactivity and Ozone Reactivity of a Proxy for Isoprene-Derived Hydroperoxyenals (HPALDs). *Phys. Chem. Chem. Phys.* **2012**, *14*, 7276–7286.
- Gierczak, T.; Burkholder, J. B.; Bauerle, S.; Ravishankara, A. R. Photochemistry of Acetone under Tropospheric Conditions. *Chem. Phys.* **1998**, *231*, 229–244.
- Blitz, M. A.; Heard, D. E.; Pilling, M. J. Study of Acetone Photodissociation over the Wavelength Range 248–330 nm: Evidence of a Mechanism Involving Both the Singlet and Triplet Excited States. *J. Phys. Chem. A* **2006**, *110*, 6742–6756.
- Horowitz, A. Wavelength Dependence of the Primary Photo-dissociation Processes in Acetone Photolysis. *J. Phys. Chem.* **1991**, *95*, 10816.
- Tadic, J. M.; Xu, L.; Houk, K. N.; Moortgat, G. K. Photooxidation of *n*-Octanal in Air: Experimental and Theoretical Study. *J. Org. Chem.* **2011**, *76*, 1614–1620.
- Singh, H. B.; Kanakidou, M.; Crutzen, P. J.; Jacob, D. J. High Concentrations and Photochemical Fate of Oxygenated Hydrocarbons in the Global Troposphere. *Nature* **1995**, *378*, 50–54.
- Wennberg, P. O.; Hanisco, T. F.; Jaeglé, L.; Jacob, D. J.; Hintsa, E. J.; Lanzendorf, E. J.; Anderson, J. G.; Gao, R. S.; Keim, E. R.; Donnelly, S. G.; et al. Hydrogen Radicals, Nitrogen Radicals, and the Production of O_3 in the Upper Troposphere. *Science* **1998**, *279*, 49–53.

- (12) El-Nahas, A. M.; Bozzelli, J. W.; Simmie, J. M.; Navarro, M. V.; Black, G.; Curran, H. J. J. Thermochemistry of Acetonyl and Related Radicals. *Phys. Chem. A* **2006**, *110*, 13618–13623.
- (13) Serinyel, Z.; Chaumeix, N.; Black, G.; Simmie, J. M.; Curran, H. J. Experimental and Chemical Kinetic Modeling Study of 3-Pentanone Oxidation. *J. Phys. Chem. A* **2010**, *114*, 12176–12186.
- (14) Sebbar, N.; Bozzelli, J. W.; Bockhorn, H. Thermochemistry and Kinetics for 2-Butanone-3yl Radical ($\text{CH}_3\text{C}(=\text{O})\text{CH}\cdot\text{CH}_3$) Reactions with O_2 . *Z. Phys. Chem.* **2011**, *225*, 993–1018.
- (15) Hudzik, J. M.; Joseph, W.; Bozzelli, J. W. Thermochemistry and Bond Dissociation Energies of Ketones. *J. Phys. Chem. A* **2012**, *116*, 5707–5722.
- (16) Lay, T. H.; Krasnoperov, L. N.; Venanzi, C. A.; Bozzelli, J. W. Ab Initio Study of α -Chlorinated Ethyl Hydroperoxides $\text{CH}_3\text{CH}_2\text{OOH}$, $\text{CH}_3\text{CHClOOH}$, and $\text{CH}_3\text{CCl}_2\text{OOH}$: Conformational Analysis, Internal Rotation Barriers, Vibrational Frequencies, and Thermodynamic Properties. *J. Phys. Chem.* **1996**, *100*, 8240–8249.
- (17) M.J. Frisch, G.W.; Trucks, H.B.; Schlegel, G.E.; Scuseria, M.A.; Robb, J.R.; Cheeseman, V.G.; Zakrzewski, J.A.; Montgomery, R.E., Jr.; Stratmann, J.C.; Burant, S.; et al. *Gaussian 03*; Gaussian, Inc.: Pittsburgh PA, 2001.
- (18) <http://www.gaussian.com/index.htm>.
- (19) Foresman, J. B.; Frisch, J. E. *Exploring Chemistry with Electronic Structure Methods: A Guide to Using Gaussian*, 1st ed.; Gaussian: Pittsburgh, PA, 1993.
- (20) Becke, A. D. Density-Functional Thermochemistry. III. The Role of Exact Exchange. *J. Chem. Phys.* **1993**, *98*, 5648–5652.
- (21) Lee, C.; Yang, W.; Parr, R. G. Development of the Colle–Salvetti Correlation-energy Formula into a Functional of the Electron Density. *Phys. Rev. B* **1988**, *37*, 785–789.
- (22) Montgomery, J. A.; Ochterski, J. W.; Petersson, G. A. A Complete Basis Set Model Chemistry. IV. An Improved Atomic Pair Natural Orbital Method. *J. Chem. Phys.* **1994**, *101*, 5900–5909.
- (23) Curtiss, L. A.; Raghavachari, K.; Redfern, P. C.; Rassolov, V.; Pople, J. A. Gaussian-3 (G3) Theory for Molecules Containing First and Second-Row Atoms. *J. Chem. Phys.* **1998**, *109*, 7764–7776.
- (24) Redfern, P. C.; Zapol, P.; Curtiss, L. A.; Raghavachari, K. Assessment of Gaussian-3 and Density Functional Theories for Enthalpies of Formation of C_1C_{16} Alkanes. *J. Phys. Chem. A* **2000**, *104*, 5850–5854.
- (25) Baboul, A. G.; Curtiss, L. A.; Redfern, P. C.; Raghavachari, K. Gaussian-3 Theory Using Density Functional Geometries and Zero-Point Energies. *J. Chem. Phys.* **1999**, *110*, 7650–7657.
- (26) Benson, S. W. *Thermochemical Kinetics*, 2nd ed.; Wiley Interscience: New York, 1976.
- (27) Ritter, E. R.; Bozzelli, J. W. THERM: Thermodynamic Property Estimation for Gas Phase Radicals and Molecules. *Int. J. Chem. Kinet.* **1991**, *23*, 767–778.
- (28) Sheng, C. Ph.D. Dissertation. Department of Chemical Engineering, Chemistry and Environmental Science, New Jersey Institute of Technology, Newark, NJ 07102; 2002.
- (29) Prosen, E. J.; Rossini, F. D. Heats of Combustion and Formation of the Paraffin Hydrocarbons at 25° C. *J. Res. NBS* **1945**, *263–267*.
- (30) Chase, M. W., Jr. NIST-JANAF Thermochemical Tables, 4th ed.; *J. Phys. Chem. Ref. Data*, Monograph 9, **1998**, 1–1951.
- (31) Furuyama, S.; Golden, D. M.; Benson, S. W. Thermochemistry of the Gas Phase Equilibria $i\text{-C}_3\text{H}_7\text{I} = \text{C}_3\text{H}_6 + \text{HI}$, $n\text{-C}_3\text{H}_7\text{I} = i\text{-C}_3\text{H}_7\text{I}$, and $\text{C}_3\text{H}_6 + 2\text{HI} = \text{C}_3\text{H}_8 + \text{I}_2$. *J. Chem. Thermodyn.* **1969**, *1*, 363–375.
- (32) Prosen, E. J.; Maron, F. W.; Rossini, F. D. Heats of Combustion, Formation, and Isomerization of Ten C_4 Hydrocarbons. *J. Res. NBS* **1951**, *46*, 106–112.
- (33) Orlov, V. M.; Krivoruchko, A. A.; Misharev, A. D.; Takhistov, V. V. Enthalpy of Vapor Phase Formation of Ketene, Ethynol, and their Analogs. *Bull. Acad. Sci. USSR, Div. Chem. Sci.* **1986**, *2404–2405*.
- (34) daSilva, G.; Bozzelli, J. W.; Sebbar, N.; Bockhorn, H. Thermodynamic and Ab Initio Analysis of the Controversial Enthalpy of Formation of Formaldehyde. *ChemPhysChem* **2006**, *7*, 1119–1126.
- (35) Sebbar, N.; Bockhorn, H.; Bozzelli, J. W. Thermochemical Properties, Rotation Barriers, and Group Additivity for Unsaturated Oxygenated Hydrocarbons and Radicals Resulting from Reaction of Vinyl and Phenyl Radical Systems with O_2 . *J. Phys. Chem. A* **2005**, *109*, 2233–2253.
- (36) Fletcher, R. A.; Pilcher, G. Measurements of heats of combustion by flame calorimetry. *Trans. Faraday Soc.* **1970**, *66*, 794–799.
- (37) Green, J. H. S. Revision of the Values of the Heats of Formation of Normal Alcohols. *Chem. Ind. (London)* **1960**, 1215–1216.
- (38) <http://rmg.mit.edu/>
- (39) Lay, T. H.; Bozzelli, J. W. Enthalpies of Formation and Group Additivity of Alkyl Peroxides and Trioxides. *J. Phys. Chem. A* **1997**, *101*, 9505–9510.
- (40) Sebbar, N.; Bockhorn, H.; Bozzelli, J. W. Structures, Thermochemical Properties (Enthalpy, Entropy and Heat Capacity), Rotation Barriers and Peroxide Bond Energies of Vinyl, Allyl, Ethynol and Phenyl Hydroperoxides. *Phys. Chem. Chem. Phys.* **2002**, *4*, 3691–3703.
- (41) <http://webbook.nist.gov>, Average of 7 values: Mosselman, C.; Dekker, H. Enthalpies of Formation of n -Alkan-1-ols. *J. Chem. Soc. Faraday Trans. 1* **1975**, *417–424*. Connell, J. E. Chemical Equilibria. 5. Measurement of Equilibrium Constants for the Dehydrogenation of Propanol by a Vapour Flow Technique. *J. Chem. Thermodyn.* **1972**, *4*, 233–237. Wadso, I. Heats of Vaporization for a Number of Organic Compounds at 25 °C. *Acta Chem. Scand.* **1966**, *20*, 544. Chao, J.; Rossini, F. D. Heats of Combustion, Formation, and Isomerization of Nineteen Alkanols. *J. Chem. Eng. Data* **1965**, *10*, 374–379. Snelson, A.; Skinner, H. A. Heats of Combustion: Sec-Propanol, 1,4-Dioxan, 1,3-Dioxan and Tetrahydropyran. *Trans. Faraday Soc.* **1961**, *57*, 2125–2131. Green, J. H. S. Revision of the Values of the Heats of Formation of Normal Alcohols. *Chem. Ind. (London)* **1960**, 1215–1216.
- (42) Sebbar, N.; Bockhorn, H.; Bozzelli, J. W. Thermochemistry and Reaction Paths in the Oxidation Reaction of Benzoyl Radical: $\text{C}_6\text{H}_5\text{C}(=\text{O})$. *J. Phys. Chem. A* **2011**, *115*, 11897–11914.
- (43) Turecek, F. (E)- and (Z)-Prop-1-en-1-ol: Gas-Phase Generation and Determination of Heats of Formation by Mass Spectrometry. *J. Chem. Soc. Chem. Commun.* **1984**, 1374–1375.
- (44) Pell, A. S.; Pilcher, G. Measurements of Heats of Combustion by Flame Calorimetry. Part 3. Ethylene Oxide, Trimethylene Oxide, Tetrahydrofuran and Tetrahydropyran. *Trans. Faraday Soc.* **1965**, *61*, 71–77.
- (45) Chao, J.; Zwolinski, B. J. Ideal Gas Thermodynamic Properties of Propanone and 2-Butanone. *J. Phys. Chem. Ref. Data* **1976**, *5*, 319–328.
- (46) Wiberg, K. B.; Crocker, L. S.; Morgan, K. M. Thermochemical Studies of Carbonyl Compounds. 5. Enthalpies of Reduction of Carbonyl Groups. *J. Am. Chem. Soc.* **1991**, *113*, 3447–3450.
- (47) Guthrie, G. B., Jr.; Scott, D. W.; Hubbard, W. N.; Katz, C.; McCullough, J. P.; Gross, M. E.; Williamson, K. D.; Waddington, G. Thermodynamic Properties of Furan. *J. Am. Chem. Soc.* **1952**, *74*, 4662–4669.
- (48) Yevstropov, A. A.; Lebedev, B. V.; Kulagina, T. G.; Lyudvig, Ye.B.; Belenkaya, B. G. The Thermodynamic Properties of β -Propiolactone, Its Polymer, and Its Polymerization in the 0–400 K Range. *Polym. Sci. USSR* **1979**, *21*, 2249–2256.
- (49) Pilcher, G.; Pell, A. S.; Coleman, D. J. Measurements of Heats of Combustion by Flame Calorimetry Part 2. Dimethyl Ether, Methyl Ethyl Ether, Methyl *n*-Propyl Ether, Methyl isoPropyl Ether. *Trans. Faraday Soc.* **1964**, *60*, 499–505.
- (50) Ruscic, B.; Pinzon, R. E.; Morton, M. L.; Srinivasan, N. K.; Su, M.-C.; Sutherland, J. W.; Michael, J. V. Active Thermochemical Tables: Accurate Enthalpy of Formation of Hydroperoxy Radical, HO_2 . *J. Phys. Chem. A* **2006**, *110*, 6592–6601.
- (51) Tsang, W.; Martinho Simoes, J. A.; Greenberg, A.; Liebman, J. F. Heats of Formation of Organic Free Radicals by Kinetic Methods in Energetics of Organic Free Radicals. Blackie Academic and Professional: London, 1996, pp 22–58.
- (52) Knyazev, V. D.; Slagle, I. R. Thermochemistry of the R-O₂ Bond in Alkyl and Chloroalkyl Peroxy Radicals. *J. Phys. Chem. A* **1998**, *102*, 1770–1778.

- (53) Sebbar, N.; Bockhorn, H.; Bozzelli, J. W. Thermodynamic Properties of the Species Resulting from the Phenyl Radical with O₂ Reaction System. *Int. J. Chem. Kinet.* **2008**, *40*, 583–604.
- (54) Kuwata, K. T.; Hasson, A. S.; Dickinson, R. V.; Petersen, E. B.; Valin, L. C. Quantum Chemical and Master Equation Simulations of the Oxidation and Isomerization of Vinoxy Radicals. *J. Phys. Chem. A* **2005**, *109*, 2514–2524.
- (55) Tokmakov, I. V.; Kim, G-S; Kislov, V. V.; Mebel, A. M.; Lin, M. C. The Reaction of Phenyl Radical with Molecular Oxygen: A G2M Study of the Potential Energy Surface. *J. Phys. Chem. A* **2005**, *109*, 6114–6127.
- (56) Sebbar, N.; Bockhorn, H.; Bozzelli, J. W. Thermochemical Similarities among Three Reaction Systems: Vinyl + O₂ – Phenyl + O₂ – Dibenzofuranyl + O₂. *Combust. Sci. Technol.* **2008**, *180*, 959–974.
- (57) Welz, O.; Klippenstein, S. J.; Harding, L. B.; Craig Taatjes, A.; Zador, J. Unconventional Peroxy Chemistry in Alcohol Oxidation: The Water Elimination Pathway. *J. Phys. Chem. Lett.* **2013**, *4*, 350–354.
- (58) Sebbar, N.; Bozzelli, J. W.; Bockhorn, H. The Oxidation Reaction of C₆HSC(=O) Radical. 6th Proceeding of the Mediterranean Combustion Symposium, Ajaccio, Corsica, France, June 7–11, 2009.
- (59) Sheng, C.; Bozzelli, J. W.; Dean, A. M.; Chang, A. Y. Detailed Kinetics and Thermochemistry of C₂H₅ + O₂: Reaction Kinetics of the Chemically Activated and Stabilized CH₃CH₂OO[•] Adduct. *J. Phys. Chem. A* **2002**, *106*, 7276–7293.